A thousand Golden Ten orbits

de Vos, J.C.

Publication date:
1994

Document Version
Publisher's PDF, also known as Version of record

Link to publication in Tilburg University Research Portal

Citation for published version (APA):
de Vos, J. C. (1994). *A thousand Golden Ten orbits*. (Research Memorandum FEW). Faculteit der Economische Wetenschappen.

Research Memorandum

Faculty of Economics and
Business Administration

Orbits

Tilburg University

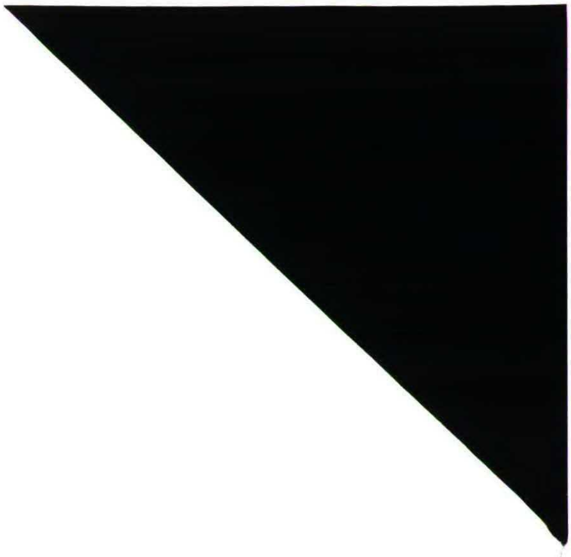

A THOUSAND GOLDEN TEN ORBITS

J.C. de Vos

FEW 654

Communicated by Prof.dr. B.B. van der Genugten

A Thousand Golden Ten Orbits

J.C. de Vos*)

Abstract

This report describes the methods used to construct a large database of accurately measured Golden Ten orbits. The contents of this database are fully set out, and from every orbit two illustrative graphs are created. The graphs enable the reader to check the orbits at a glance.

The concerning data will later be used as a basis for further research. By fitting physical and stochastical models to empirical data, we will hopefully get a better understanding of the nature of the effects that determine the outcome of the Golden Ten game.

Keywords and Phrases

Central projection, digital image processing, Golden Ten, particle tracking.

*) Samenwerkingsorgaan Brabantse Universiteiten (SOBU),
P.O. box 90153, 5000 LE Tilburg / P.O. box 513, 5600 MB Eindhoven,
The Netherlands.

Table of contents

1 General introduction 1

2 Problem definition 5

3 The experimental setup 7

4 The theory of central projection 11

5 Mastering DigImage 15

6 Calibrations 17

- 6.1 Estimation of the image transormation 17
- 6.2 Shifting the image 20
- 6.3 Correcting the time code 24
- 6.4 The final transformation program 24

7 Experimental results 27

- 7.1 Physical dimensions 27
- 7.2 Environmental conditions 28
- 7.3 Time series 29
- 7.4 Data storage 30

8 Literature 33

A Tracking parameters 35

B Transformation program 37

C Environmental data 43

D Example graphs 75

E Example file 79

1 General introduction

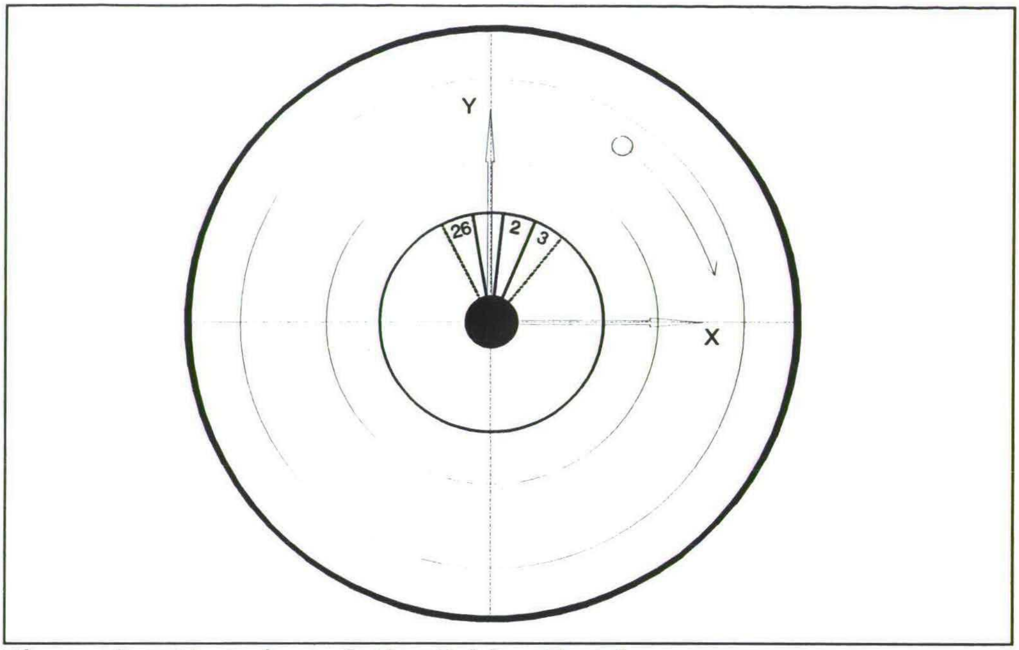

Figure 1a. Top-view of the Golden Ten drum.

Golden Ten is a modified version of Roulette. The game is played with a small ball moving in a relatively large bowl, at the bottom of which there is a ring with numbered compartments (see Fig. 1a). The players can not effect the motion of the ball; all they can do is stake money on one or more possible outcomes. The main differences with roulette are that the large bowl is in fact a smooth, conic drum (see Fig. 1b), in which the ball is smoothly spiralling down, and - secondly - that the players do not have to stake before the ball has reached a certain level. It is claimed that the possibility to observe part of the ball's orbit enables an experienced player to make a better than random guess on the outcome, thus implying that Golden Ten is a game of skill, rather than a game of chance.

From previous research by van der Genugten and Borm (1991) we know that the motion of the ball in the drum is certainly not deterministic, as would have been the case if the factors that determine this motion were fixed and not subject to small fluctuations and (probably) random perturbations: different experiments often show remarkable

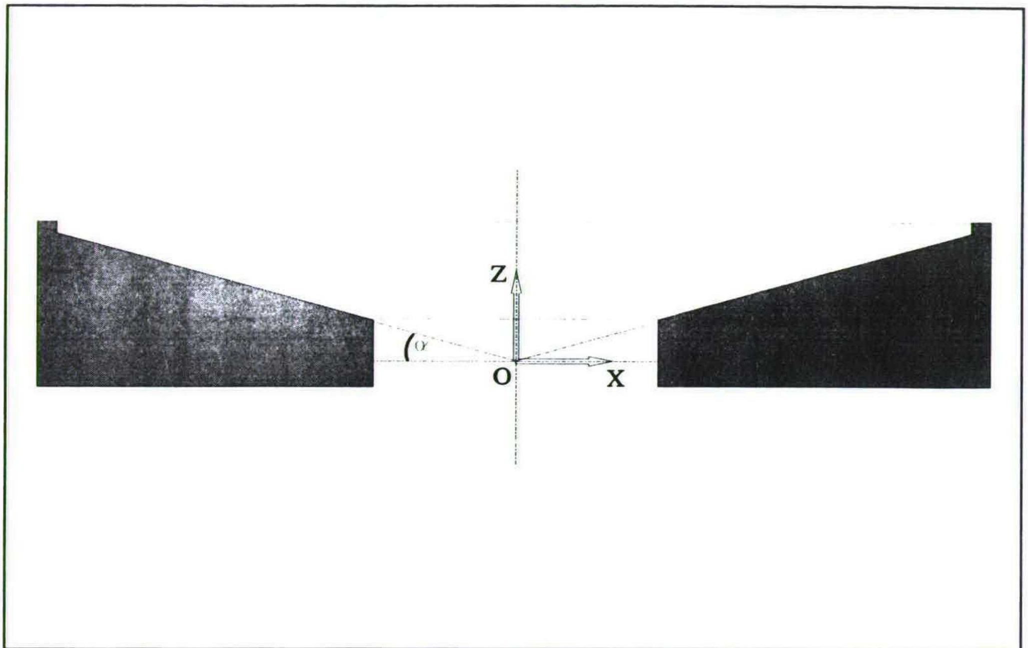

Figure 1b. Side-view of the Golden Ten drum (cross-section).

dissimilarities. The only way to gather more information about the nature of these fluctuations and perturbations is to conduct a large number of experiments, and simply measure the orbits of the ball. A large number of accurately measured orbits allows for a thorough comparison of classical mechanical models on the one hand, and extensions of these models with random components on the other. In the end, we hope to acquire an appropriate model for describing and predicting the motion of the ball in the drum.

The data from the above-mentioned previous research in 1991 would have been a perfect basis for further research. However, the database turned out to be very difficult of access, and the concerning data appeared not to meet our requirements of accuracy. For these reasons, we decided to conduct an extra thousand experiments - in june 1993 - at the Laboratory of Mechanical Engineering at Eindhoven University of Technology. The measurements were later processed at the division of Fluid Dynamics & Heat Transfer, Department of Technical Physics. The final elaboration of the data took place at the Department of Econometrics at Tilburg University. This last activity turned out te be much more laborious than foreseen, and could not be completed until april 1994.

This report describes the way in which the experiments were set up and conducted, and it summarizes the experimental results. The results will later be used as a basis for further research.

I hereby wish to thank the people who helped me in my hunt for the data. First of all, I would like to thank Gert-Jan van Heijst and Gert van der Plas, who leased me their computer system to digitize the recorded experiments. I am also much obliged to Gerrit Peters for introducing me to the lab, to Leo Wouters and Theo van Duppen for letting me use their video equipment, and to Sjef Garenfeld for helping me to build a construction to fix the camera. Furthermore I owe special thanks to Rens van Mierlo for designing an ingenious illumination setup, and to Christel Nooijen for constructing the studio booth.

2 Problem definition

According to classical mechanical theory, the motion of the ball is completely determined by the forces that act on it. The forces in their turn depend on the physical characteristics of the ball itself, those of the drum and of the environment in which the game is played. These characteristics can be divided into two categories: those that can be measured directly, and those that have to be measured indirectly, i.e. derived by means of a mechanical model. The environmental conditions can even be harder to determine, especially factors like "presence of dust particles on the drum surface", or "greasy fingerprints on the ball".

The dimensions of the drum can be measured by means of some suitable instrument; this also applies to the radius and the mass of the ball. The air temperature - one of the environmental conditions that may have its influence on the experiments - can also be measured directly. Other environmental factors can only be measured by fitting an appropriate theoretical model to experimentally acquired data; some of the secondary characteristics - like "strange sounds" and "heavy traffic passing by" - may however sometimes be noticed by mere observation.

The main goal of our experimental setup was to collect a large number of accurately measured ball orbits, together with as much additional environmental information as possible. Each orbit should consist of a long time series of (two dimensional) ball coordinates. A large database of orbits is the only guarantee for an accountable, statistically based comparison of theoretical models with empirical data.

3 The experimental setup

First of all we had to be sure that, during the experiments, the drum was permanently in a perfect horizontal position. To achieve this, we installed the drum on a solid tripod and waited for a couple of days for the drum to settle. After that, the position was adjusted by means of a straight metal bar and a levelling instrument with an accuracy of 0.05 mm per m. The dimensions of the drum were measured with a marking gauge, moving over the before mentioned straight metal bar, and a spring rule. The marking gauge was also used to measure the diameter of the ball, and the weight was measured with a scale.

As a tracking system for the ball we used a computer system for digital image analysis. Because this type of systems requires a sharp contrast between the object to track and its background, a major problem was raised here: the colour of the ball is whitish and the surface of the drum is bright unpolished steel! This problem was tackled by designing a special illumination setup: in a large black flannel tent a ring of light bulbs was placed just outside and above the rim of the drum. The shadow of the rim prevented the surface to reflect any light, and only the top half of the ball was illuminated. A cardboard cylinder in the centre of the drum granted an even distribution of light, whereas adhesive black felt prevented the rim to reflect. The tops of the light bulbs were covered with black cardboard, so that the bulbs would not come into vision when the total configuration was looked upon from above. At four points along the rim of the drum we attached a small light bulb; these four lights served as marker points for the computer system.

Perpendicular above the centre of the drum we fixed a Panasonic F10 CCD-camera to register the orbits. The camera images were recorded on Super VHS tape (of type PDM-625) by using the available Panasonic AG-6200 video tape recorder. The recorded image was checked on-line with TIM software, version 3.36, running on a 386 personal computer with 3 MB of extended memory and a PCVISIONplus frame grabber expansion board. This computer system did not allow for real-time image analysis, it merely functioned as a means to check for possible changes in illumination or camera position. The experiments could later be identified trough the numbered notes that were placed in the lower right corner of the image.

After the recordings, the images were digitized and analysed with DigImage software version 1.2, running on a 486 personal computer with a DT-2861 frame grabber expansion board and 8 MB of extended memory, connected to a Panasonic AG-7350 super VHS video tape recorder. Although DigImage was especially designed for image processing of fluid dynamics, we found that it was also capable - with a suitable adjustment of the system parameters - to trace one or more white balls in a dark environment. After being processed by DigImage, the data were further transformed and modified with SAS software version 6.04. SAS is a statistical package with a considerable amount of data management tools; it was run on a 486 personal computer with 2 MB of expanded memory.

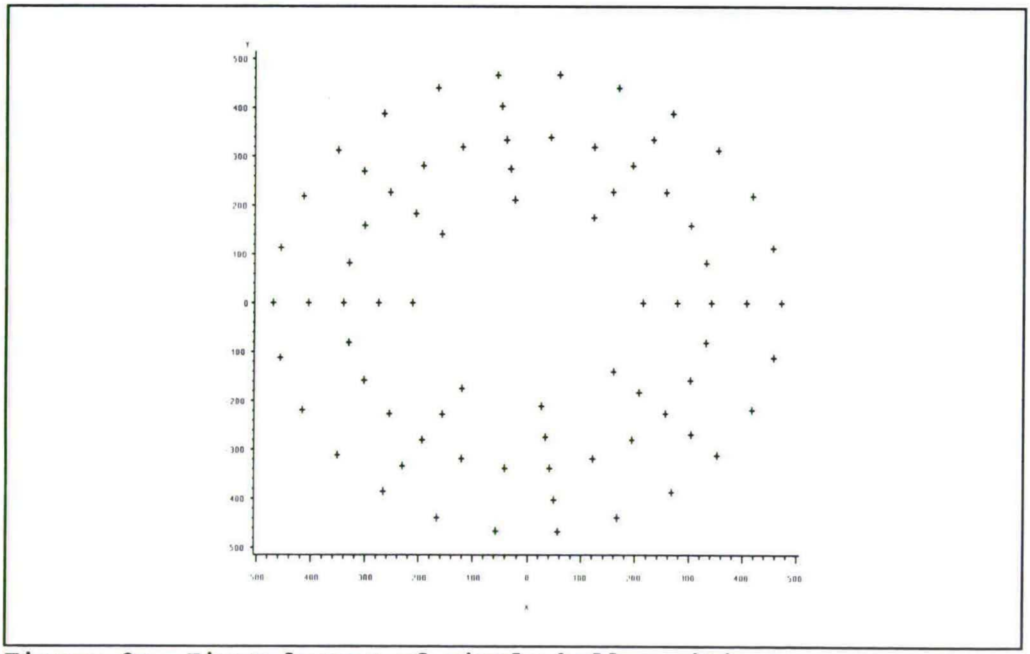

Figure 2a. First layout of single ball positions.

In spite of our meticulous preparations, we did anticipate some deformation and variation in our recorded images. For this reason we designed two (slightly different) layouts of single ball positions. These positions were measured directly by means of a straight wooden ruler, as well as indirectly by the computer system. One layout was laid down and recorded before the experiments were carried out, the other afterwards. By recording two series, we

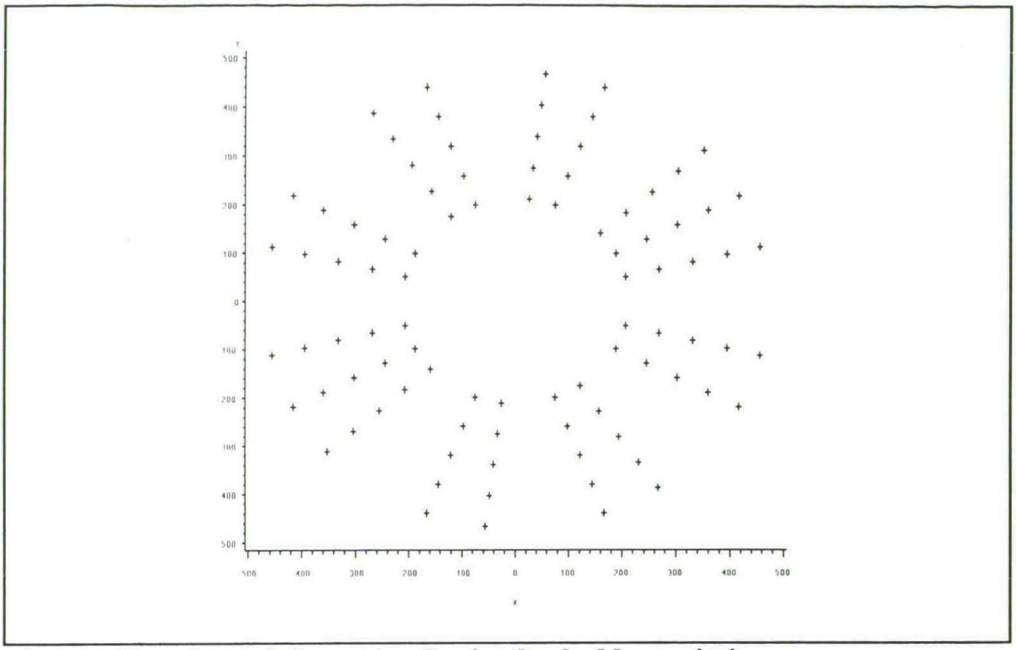

Figure 2b. Second layout of single ball positions.

acquired a means to check for changes in the environmental conditions during the experiments. The resulting pairs of measurements for both layouts were meant to serve as a mapping function from the recorded images to real-world coordinates. The layouts are plotted in Figs. 2a and 2b.

In order to be able to eliminate possible secundary effects - like cleaning effects and effects of different balls or different video tapes - we devided our experiments into thirty runs of (approximate) size thirty-five. The video tapes were changed after every two runs, and the ball was changed after every set of six runs. At the beginning of each run, the drum as well as the ball were cleaned with alcohol. The ball was regularly cleaned with a dry paper towel, and was only touched with special, clean gloves. For every experiment we recorded (on paper) the temperature of the air at the beginning of the experiment, the outcome of the experiment, any audible or visible irregularities, possible variations in the launching of the ball, and irregularities during the fall into the numbered compartments.

4 The theory of central projection

The recordings consist of a large number of images of a ball moving in a three dimensional object space, which is bounded by the drum. Every image is a perspective tranformation of this object space: it is the result of a projection through a system of lenses on the image plane of the camera. This tranformation can be found by applying the theory of central projection, which is usually condensed into the *collinearity principle*: every point in the object space can be connected to exactly one point in the image space by means of a straight line through the centre of projection (see Schwidefsky and Ackermann, 1976).

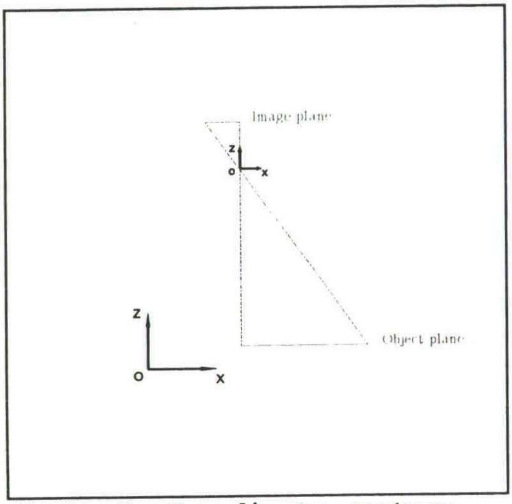

Figure 3. Coordinate systems.

To determine the coordinates in the object space, we use a Cartesian coordinate system $\{O_{XYZ}\}$ (see Fig. 1). For the coordinates in the image space, we use a similar system $\{o_{xyz}\}$, where o is the centre of projection, lying just below the image plane (see Fig. 3). The x- and the y-axis are fixed by DigImage, but for the X- and the Y-axis we still have full freedom of choice. By choosing these axis as in Fig. 1, we let X, Y and Z respectively point in (almost) the same direction as x, y and z.

In an ideal setup - where the illumination is perfectly uniform, and $\{o_{xyz}\}$ is a translation of $\{O_{XYZ}\}$ - we have the simple set of relations

$$\begin{cases} \dfrac{X-X_0}{Z-Z_0} = \dfrac{x}{-c} \\ \dfrac{Y-Y_0}{Z-Z_0} = \dfrac{y}{-c} \end{cases}, \qquad (1)$$

where (X_0,Y_0,Z_0) are the coordinates of the centre of projection o in the system $\{O_{XYZ}\}$, and c is the distance from o to the image plane. The constant c is usually called the *camera constant*. In a more general setup - where the illumination is still uniform, but the $\{o_{xyz}\}$ system may have been rotated and rescaled, we have a more intricate set of equations,

$$\begin{cases} \dfrac{X-X_0}{Z-Z_0} = \dfrac{a_{11}x+a_{12}y-a_{13}c}{a_{31}x+a_{32}y-a_{33}c} \\ \dfrac{Y-Y_0}{Z-Z_0} = \dfrac{a_{21}x+a_{22}y-a_{23}c}{a_{31}x+a_{32}y-a_{33}c} \end{cases}, \tag{2}$$

where $\{a_{ij}\}$ is the matrix of successive rotations over ω, φ and κ around the x-axis, and the rotated y- and z-axis, respectively:

$$\{a_{ij}\} = \begin{bmatrix} \cos\varphi\cos\kappa & \cos\omega\sin\kappa+\sin\omega\sin\varphi\cos\kappa & \sin\omega\sin\kappa-\cos\omega\sin\varphi\cos\kappa \\ -\cos\varphi\sin\kappa & \cos\omega\cos\kappa-\sin\omega\sin\varphi\sin\kappa & \sin\omega\cos\kappa+\cos\omega\sin\varphi\sin\kappa \\ \sin\varphi & -\sin\omega\cos\varphi & \cos\omega\cos\varphi \end{bmatrix}. \tag{3}$$

Scaling factors automatically cancel out, provided that the camera constant is measured in the same units as the distances in the image plane itself.

A non-uniform distribution of light can seriously deform the camera image. This is also true - to a lesser extent - for uncertain factors like fluctuations in the power supply, weak spots in the magnetic video tape, warming-up effects in the computer hardware, etc. Without further knowledge of the nature of these effects, it is impossible to find an exact relation between the image and the real world. The most obvious way to proceed is to allow for more variation in the parameters in (2). For estimation of the desired mapping function, we will therefore use equation set (4), with more general parameters $\{b_{ij}\}$,

$$\begin{cases} \dfrac{X-X_0}{Z-Z_0} = \dfrac{b_{11}x+b_{12}y+b_{13}}{b_{31}x+b_{32}y+b_{33}} \\ \dfrac{Y-Y_0}{Z-Z_0} = \dfrac{b_{21}x+b_{22}y+b_{23}}{b_{31}x+b_{32}y+b_{33}} \end{cases} \quad (4)$$

The only constrained parameter in (4) is b_{33}: we will use it as a scaling factor for the rest of the parameters.

5 Mastering DigImage

DigImage is an image processing system that consists of several modules, one of which is especially designed for particle tracking. This last module enables the user to trace up to 4095 white particles in a dark background, and to track them for an arbitrary long period of time. The user can change a number of system parameters to adjust the tracking program to different experimental setups. Attachment A contains a listing of the settings we used. Only the first three parameters (file name, experiment name, and total tracking time) were varying from experiment to experiment, the other parameters were fixed.

Because of possible synchronisation errors - which are due to the technical limitations of both the video tape recorder and the frame grabber board - DigImage will only process video tapes that contain special audio pulses. These pulses can be added to the tape after the images have been recorded. Optimally recorded audio pulses - requiring a tape of a better than average quality - guarantee a 100% reliable timing (Dalziel, 1992).

After an image has been captured, DigImage searches the image for the (user defined) permanent reference points. In our setup these points were the four small light bulbs on the outside of the drum. After the reference points have been identified, the captured image is shifted over an integer number of positions, in order to match the user defined points as good as possible. If the differences fall within certain limits, the image is kept and further analyzed; otherwise the image is dropped and recaptured. All this implies that the difference between the analyzed image and the real-world situation is small, but still subject to certain perturbations. This is especially true in our situation, since the small light bulbs appeared not to be fastened tightly enough to prevent them from slight sagging.

During the analysis phase, DigImage searches the image for particles. Each particle is compared to every particle in the previous image, and only those particles that seem to match, are considered for further tracking. During the experimental phase we found that at least two balls are needed before any matches can be found. We fixed this problem by placing a non-moving ball on top of a small cylinder, positioned right above the top of the drum. Furthermore it appeared that the moving ball could only be tracked for exactly one time step. This was long enough for the system to save the corresponding coordinates, but not long enough to allow us to use any more of the available tracking utilities.

Eventually we were able to generate from every series of experiments a set of four files of which the first serves as an index to the second, and the second contains the ball coordinates (usually of both balls). The record structure of the first file is thus that the record numbers correspond to the total elapsed time, and that the two next numbers are the corresponding record numbers in the second file. The second file is a direct access binary file containing two-byte, unsigned integer values, representing rescaled ball coordinates. We used SAS software to read these two files and to combine them, thus to render a time series of ball coordinates.

Two-byte, unsigned integer values range from 0 to 65535, whereas video screen coordinates - which are measured in rectangular *pixels* - range from 0 to 511 (horizontally and vertically). DigImage rescales the pixels coordinates to a user defined, rectangular tracking window, and then rescales them again to user defined world coordinates (see Dalziel, 1992). The coefficients of the first mapping function - which is a linear transformation - can be found in the third tracking file. The coefficients of the second transformation are recorded in the fourth file; they should represent the mapping function that was described in equation set (4). However, since none of the offered alternatives matched, we chose not to use this feature. But sometimes we accidentally did use it - in which case we used a reflection of coordinates - so we had to check the last tracking file as well.

Note that due to the restricted lease contract, we were not allowed to analyze more that four tapes. On these four tapes we recorded 350 experiments, which is approximately one third of the total number. The rest of the experiments still remains available on tape, but from these experiments only some very basic information has been subtracted.

6 Calibrations

6.1 Estimation of the image transformation

The twelve unknown coefficients of the non-linear mapping function in equation set (4) can be estimated with the data from the two layouts in Figs. 2a and 2b. However, because of some small changes in illumination, and because of the sagging reference lights, we expect the results for the two layouts to be slightly different. To eliminate possible start-up effects, we use the second layout for the actual estimation, and the first layout to check the results.

Although we do not impose any constraints on the parameters $\{b_{ij}, (i,j) \neq (3,3)\}$, we do want to check the estimations with the original formulae in equation (3), in order to get some idea of the errors we make. This requires first of all an estimation of the *aspect ratio*: the ratio of horizontal to vertical size of the pixels that compose the image. Since an incorrect aspect ratio would deform an actual circle to an apparent ellipse, we use the equation

$$\left(\frac{x-x_0}{\lambda}\right)^2 + \left(\frac{y-y_0}{\mu}\right)^2 = 1 \qquad (5)$$

and a simple least squares procedure, to fit an ellipse to the first round of the ball on every one of the four tapes. Note that (x_0,y_0) is the midpoint of the (apparent) ellipse, and λ/μ is the ellipticity. Although this method does not take into account the deformations due to equation set (4), the resulting estimate of $\mu/\lambda = 1.447 \pm 0.001$ turns out to be accurate enough to serve our purpose.

After multiplying the x-coordinate with 1.447, we proceed by simultaneously fitting the equations in (4) to the data from layout number two. Since equation (3) implies that the estimates of a_{11} and a_{22} should be close to one, we fix the value of b_{33} to -1802.5764, thus causing the corresponding estimates of b_{11} and b_{22} to be as close to 1 as possible. The results of the estimation procedure are presented in Table 1 (where distances are expressed in millimeters and angles in radians). The estimated 95% confidence intervals in this table indicate a relatively large inaccuracy, but the residual plots in Figs. 4 and 5 - where the

Table 1: estimated coefficients.

Parameter	Estimate	Asymptotic Std. Error	Asymptotic 95 % Confidence Interval Lower	Upper
X0	105.592291	60.76114623	-14.3575723	225.5421549
Y0	-305.620485	76.97893737	-457.5862328	-153.6547368
Z0	3788.291936	629.22828644	2546.1190702	5030.4648010
B11	1.003212	0.16828105	0.6710048	1.3354191
B12	0.001356	0.00145866	-0.0015233	0.0042358
B13	-82.386070	28.37007459	-138.3920346	-26.3801063
B21	0.004365	0.00095288	0.0024834	0.0062456
B22	0.996788	0.16819614	0.6647481	1.3288272
B23	145.803185	27.64348536	91.2315957	200.3747737
B31	-0.046473	0.00576468	-0.0578527	-0.0350923
B32	0.088860	0.00576032	0.0774881	0.1002312

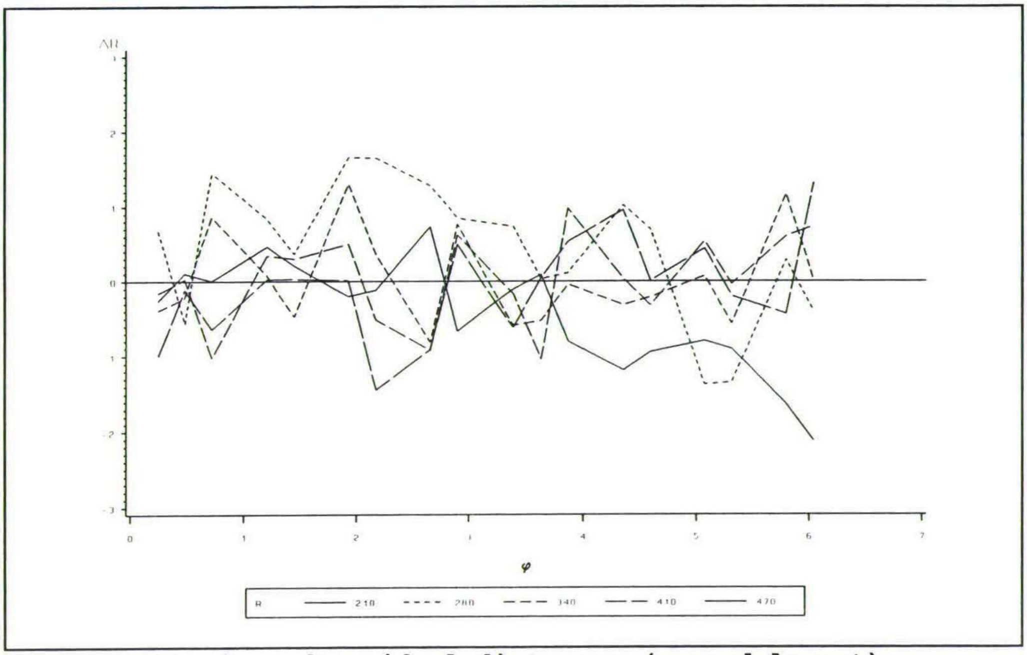

Figure 4. Estimated residual distances (second layout).

position of the ball is expressed in polar coordinates (R,φ) in the xy-plane - show that the errors are not systematic, except maybe for the innermost region of the drum, near compartments 11/12 and 15/16. In the first region we seem to overestimate the distance R, in the second we seem to underestimate the angle φ.

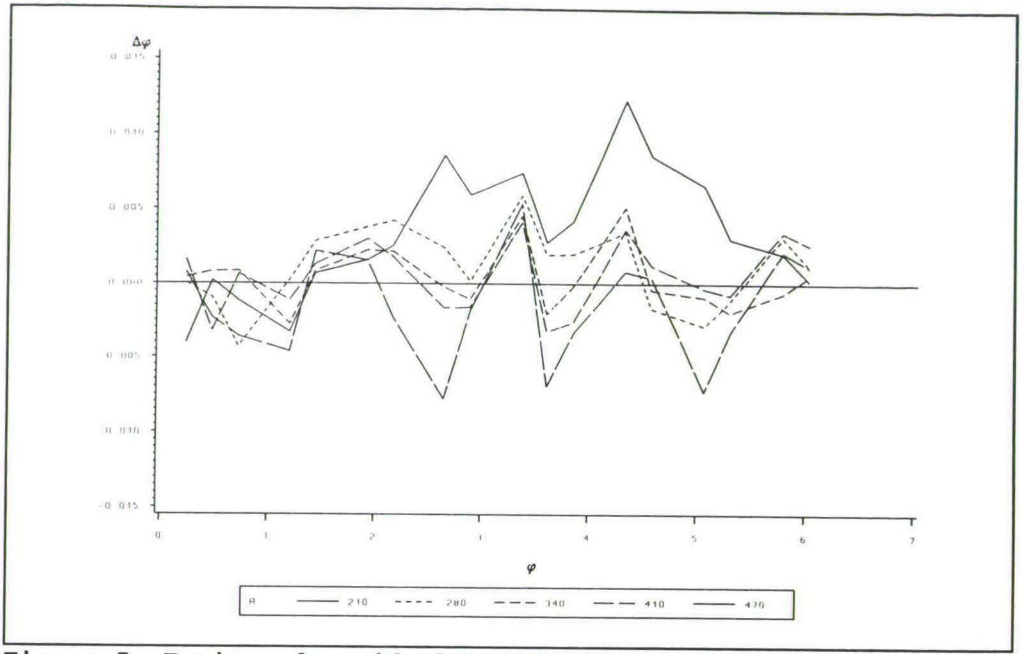

Figure 5. Estimated residual angles (second layout).

Table 1 also indicates that the camera and illumination setup were far from ideal. From the estimated values of X_0 and Y_0 we find that the camera may have been positioned at more than 30 centimeters distance from the main axis of the drum. We also find - from the estimated b_{32}, b_{31} and b_{21} - that the camera was probably rotated around the x-, the y- and the z-axis over the respective angles 0.09, -0.05, and 0.004 radians.

Application of the estimated transformation to layout number one, results in the somewhat surprisingly shaped graph in Fig. 6. The rough sine shape is caused by two effects: one is the sagging of the four reference lights (which is in fact a warming-up effect), the other is a warming-up effect of the computer hardware: since we knew the lights sagged, we redefined our four reference points at the beginning of each computer run, thus superimposing an extra shift on the data. We can try to eliminate both effects by shifting the data back into the proper direction, but since the recorded orbits are also afflicted with this defect, and because the orbits contain much more data than the layouts, we apply the shift directly to the orbits themselves.

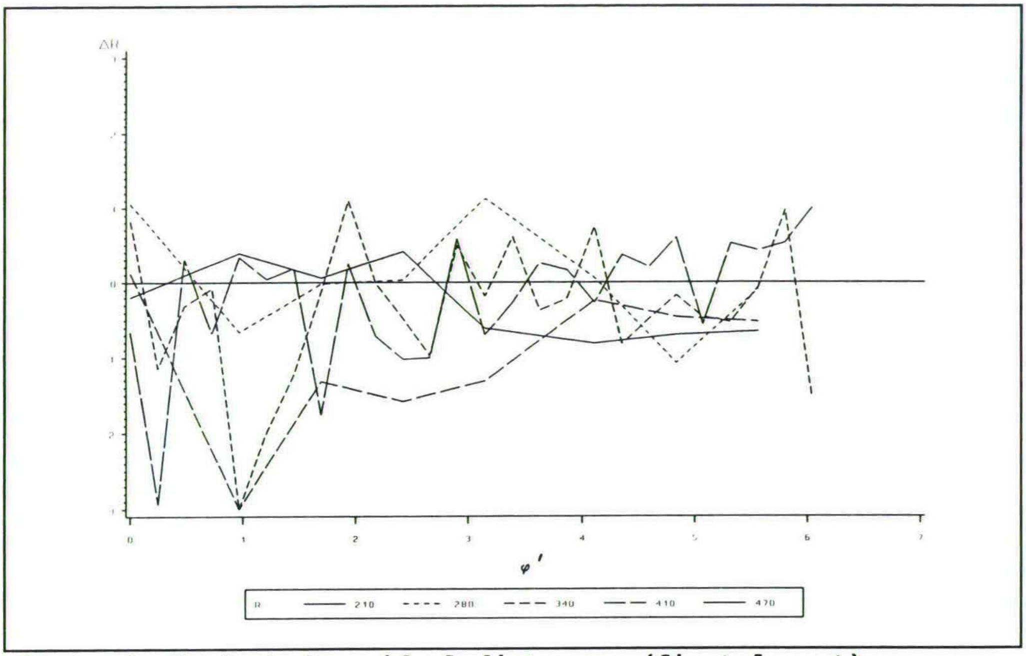

Figure 6. Estimated residual distances (first layout).

6.2 Shifting the image

The mapping function in equation set (4) can be rewritten as

$$\begin{cases} X = X_0 + (Z - Z_0)\,\dfrac{b_{11}x + b_{12}y + b_{13}}{b_{31}x + b_{32}y + b_{33}} \\ Y = Y_0 + (Z - Z_0)\,\dfrac{b_{21}x + b_{22}y + b_{23}}{b_{31}x + b_{32}y + b_{33}} \end{cases} . \tag{6}$$

Given matrix $\{b_{ij}\}$ and vector $(X_0,Y_0,Z_0)'$, we have at our disposal a mapping function from (x,y,z) to (X,Y,Z), provided that we also know Z. For the centre of the ball, this third coordinate equals

$$Z = \sqrt{X^2 + Y^2}\,\tan\alpha + \frac{a}{\cos\alpha} , \tag{7}$$

since the ball is constrained to move on the surface of the drum; the angle of inclination of this surface is denoted with α, and the radius of the ball with a. The second factor in (7) can be eliminated by adding the same factor to Z_0, as we in fact already did to obtain the results in Table 1. For constant α we use the value atan(1/12), see Section 7.1. Substitution of (7) into (6) yields a system of two quadratic equations in the two unknowns X and Y. This system can be solved by requiring that the value of Z must always be greater than zero.

This leaves the problem of estimating the shift caused by the two warming-up effects. For every orbit, we estimate this effect by using the first round of the ball along the rim. We know that this round is a perfect circle with a radius of 470 mm (see Section 7.1), so we estimate the shift (x_s,y_s) by using the equation

$$470^2 = \left\{X_0 + \left(\frac{470}{12} - Z_0\right) \frac{b_{11}(x-x_s) + b_{12}(y-y_s) + b_{13}}{b_{31}(x-x_s) + b_{32}(y-y_s) + b_{33}}\right\}^2 + \left\{Y_0 + \left(\frac{470}{12} - Z_0\right) \frac{b_{21}(x-x_s) + b_{22}(y-y_s) + b_{23}}{b_{31}(x-x_s) + b_{32}(y-y_s) + b_{33}}\right\}^2 , \tag{8}$$

and minimizing the sum of squared errors. We then subtract from the resulting estimates the corresponding values we find when we use the first eightteen data points of the second layout (these eightteen points are also positioned along the rim). The residual distances from this procedure appear to show the same error structure as in Fig. 4; Fig. 7 shows the corresponding structures for both the second layout, and an arbitrary orbit (T15B02, see Section 7). Note that the horizontal axis respresents the estimated angle φ', not the actual angle φ.

The encouraging results invite us to also try to shift the images of the first layout, thus allowing for a visual comparison of layouts number one and two. This is a somewhat precarious endeavor though, since we have only twenty-four data points at our disposal, some of which have not exactly been positioned along the rim. Figure 8 shows the results. By comparing Figs. 4 and 8, we find that the residual distances roughly have the same structure, except for the outermost region of the drum near compartments 03/04. This deviation can be caused by illumination effects, but it can also be produced by our

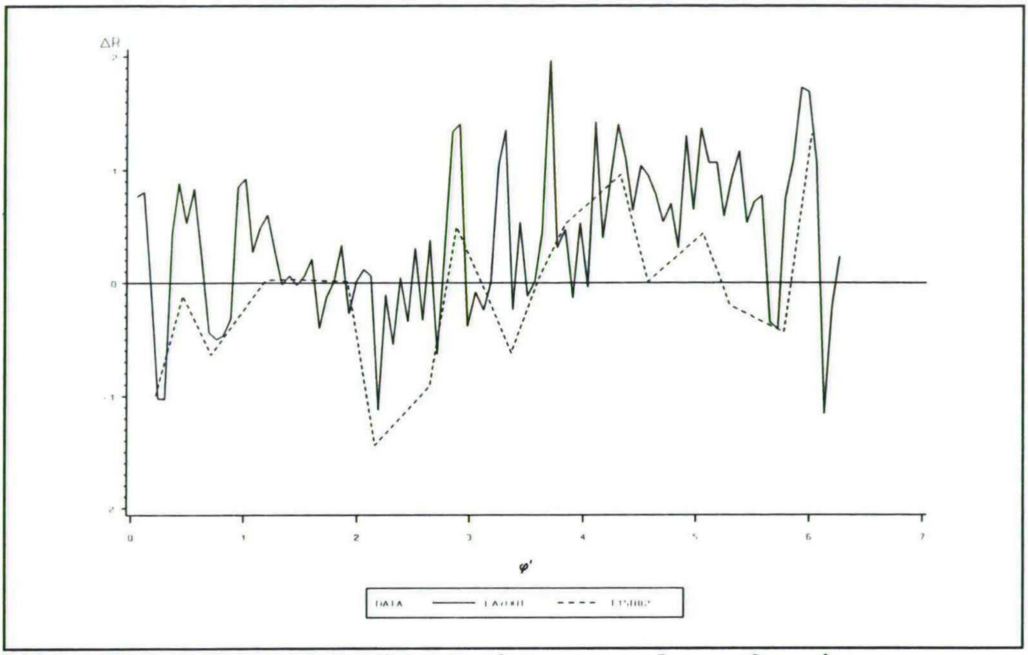

Figure 7. Estimated residual distances along the rim.

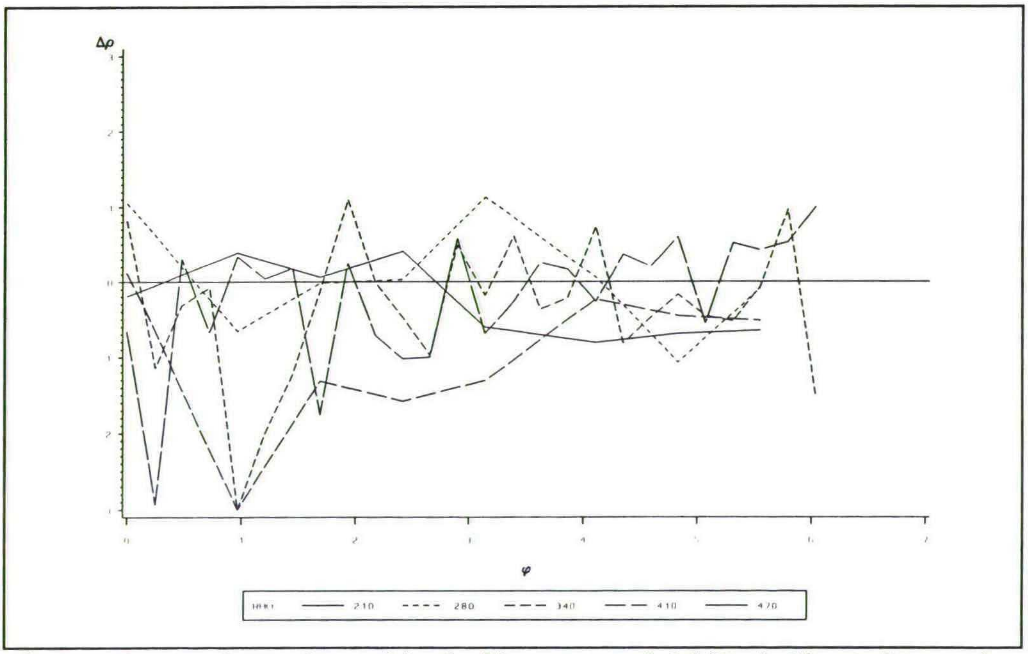

Figure 8. Estimated residual distances (shifted first layout).

measurement method.

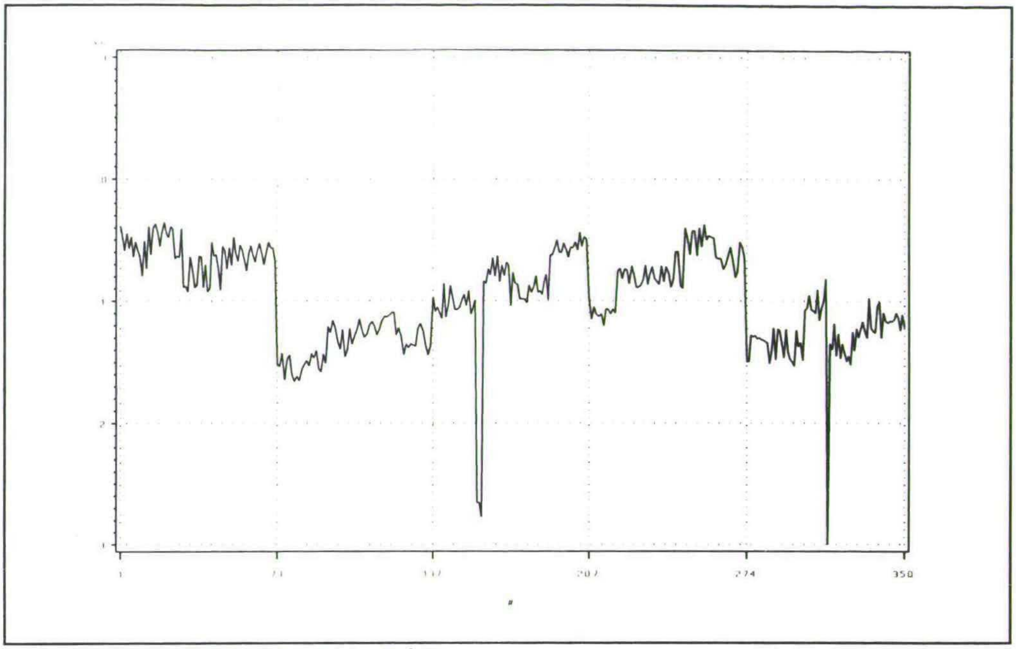

Figure 9a. Estimated x-shifts.

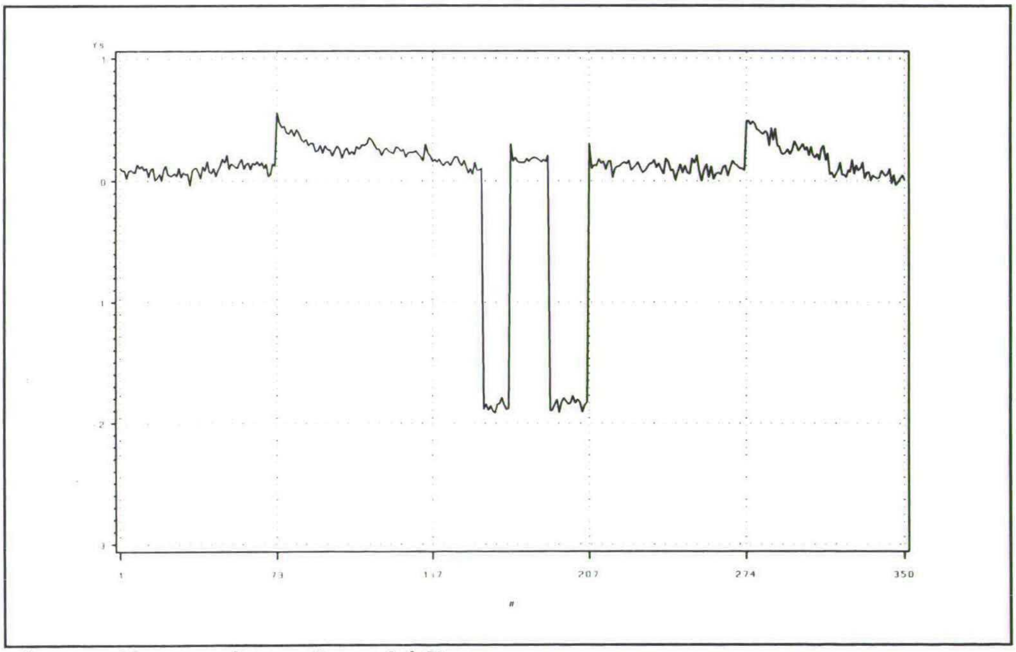

Figure 9b. Estimated y-shifts.

One last remark on the estimated shifts. In Figs. 9a and 9b we plotted the estimated x- and y-shift (in pixels) against the experiment number. The vertical lines in the graph indicate a change of tapes. Besides the two warming-up effects, two other effects are revealed here: a tape effect (when crossing the vertical lines), and an effect caused by the tracking software, appearing as an extra shift over exactly one or two positions.

6.3 Correcting the time code

The last complication we encountered when composing the time series was brought on by the unexpectedly large time code errors. As stated before in Section 5, the tracking program produces a file containing an indicator of the total elapsed time. Since the quality of our tapes was only just average, the timing of the system appeared to be quite messy. The errors were eventually coped with in two steps.

First, we checked every fifteenth record number, since at these numbers the system paused to rewind and replay the tape. We then used a rough estimator to predict the next ball position, and used the difference between the predicted and the actual position to correct the time code. This algorithm performed reasonable well, but we still had to use a second step, during which we plotted the approximate angular velocity $\Delta\varphi/\Delta t$ against the total covered angle φ, and watched for conspicuous anomalies. The remaining errors were corrected manually.

During this process we found that the time code errors ranged from -0.16 to +0.08 seconds, depending on the tape number. Furthermore, tape number 12 appeared to contain four exeriments that were too messy to correct. There also appeared to be one such experiment on tape number 15. See Section 7.3.

6.4 The final transformation program

Attachment B contains a listing of the SAS program we used to transform the raw data into the required time series. First of all, this program reads the user supplied filenames, and then it reads the corresponding four data files. It then merges the files, and removes the positions of the non-moving ball. After this - while counting the number of subsequent experiments - it tries to correct the time codes as good as possible. Next, it splits off the different experiments, and for every experiment it uses the first round to estimate the shift.

It finally applies the estimated shift, produces two graphs for every orbit, and writes a simple ASCII file. See also SAS Institute (1987), and De Vos et al. (1990).

7 Experimental results

7.1 Physical dimensions

We experimented with five different Golden Ten balls. The measurements of these balls are summed up in Table 2a. The estimated mean values of the radius and the weight of the ball are found to be 17.45 mm, and 38.3 gr. The corresponding 95% confidence intervals are (17.43 mm, 17.47 mm) and (37.9 gr, 38.7 gr).

Table 2b sums up the measurements for the dimensions of the drum. Note that the observation ring and the limit ring are two special grooves on the surface (their position is used to determine when the players can start or have to stop the betting). The diameters have all been measured in the xy-plane (see Fig. 1a). Furthermore note that the estimated angle of inclination of the drum surface is very close to atan(1/12). Since the drum was manufactured on a lathe, we can assume that this lathe was adjusted to a ratio of exactly 1/12.

Table 2a: physical dimensions of the five balls.

dimension	estimated values	accuracy	unit
diameter	34.895, 34.895, 34.925, 34.875, 34.905	0.005	millimeters
mass	38.2, 38.2, 38.5, 38.1, 38.4	0.2	grams

Table 2b: physical dimensions of the drum.

dimension	estimated value	accuracy	unit
outer diameter	974.0	0.5	millimeters
observation ring	760.0	0.5	millimeters
limit ring	518.0	0.5	millimeters
inner diameter	410.0	0.5	millimeters
angle of inclination	0.0831	0.0003	radians

7.2 Environmental conditions

As was stated before in Section 2, we have tried to collect as much environmental information as possible. In Attachment C we summarized the concerning data in a table of 1042 experiments, grouped together by the tape they were recorded on. The experiments were coded from T01B01 to T15B77: the first number - ranging from 01 to 15 - indicates the tape (T for Tape), and the second number - roughly ranging from 01 to 70 - identifies the experiment (B for Ball).

The second and third column of the table respectively report the outcome of the experiment, and the air temperature (in degrees Celsius). The fourth column represents some - unfortunately unavoidable - changes in the setup, the fifth column indicates the quality of the launch, and the last column reports possible recording errors. The rest of the columns indicate observed (mostly audible) irregularities.

The first irregularity column indicates an eventual collision with a compartment lamella; furthermore there is a column for the code of the irregularity, two for the roughly estimated position (in polar coordinates) of a removed speck of dust, four columns for two audible local irregularities, five columns for irregular rounds, and finally one column for an entire irregular band. The codes for these changes, errors and irregularities are explained in Table 3.

At the end of experiment T01B17, we discovered that the compartment ring was slightly thrusting out above the drum surface, so we readjusted the position of the ring at the beginning of T01B18 (as can be seen in Attachment C). This implies that the first seventeen experiments are largely unusable.

Table 3: codes for environmental changes.

code	launch	setup	lamella	irregularity	recording error
1	firm	surface cleaned	along	stain on drum	booth not closed
2	limp	ball changed	against	drill in lab	speck on rim
3	with side	compartment ring adjusted	across	speck on ball	fluctuating camera
4	ideal	reference light adjusted	-	speck on drum	light ring pushed
5	-	iris adjusted	-	skid along rim	power fault
6	-	camera switched off, on	-	odd orbit	wrong numbered note
7	-	tape recorder adjusted	-	-	-

7.3 Times series

Out of the above-mentioned 1042 experiments we have eventually extracted 350 time series of ball coordinates. The coordinates are expressed in polar coordinates, with the sign of the total covered angle consequently flipped over, since the ball was rolling in the opposite direction (i.e. clockwise). From every time series we produced two graphs: both the distance R and the approximate angular velocity $\Delta\varphi/\Delta t$ are plotted against the total covered angle φ. In Attachment D we displayed the two graphs for the first available experiment (T10B03). Since adding the rest of the graphs would extend Attachment D with an extra 698 pages, we decided to move these graphs to two supplementary reports. These two additional reports can be obtained from the author of the main report.

As can be seen in Figs. 4 and 5, we know that the errors in the distance R approximately range to $\pm$ 2 mm, and those in the angle φ roughly to $\pm$ 0.01 rad. Furthermore we can deduce from the first graphs of experiments T11B65 and T12B24, that the corresponding orbits have not been processed to their full extent. From the second graphs of T12B12, T12B22, T12B25, T12B55, and T15B40, we also learn that the time codes for these orbits are very unreliable (although the errors do not seem to be systematic).

7.4 Data storage

The data concerning the environmental conditions are electronically stored as a SAS data set, named ENVIRONM.SSD. The structure of this file is given in Table 4.

All the above-mentioned 350 orbits are accessible through DigImage files, as well as through 350 corresponding ASCII files. The names of the ASCII files exactly match the names of the experiments; the extensions all equal "DAT". As an example, we included in Attachment E a listing of the first and the last part of T10B03.DAT. The general structure of the files is described in Table 5. Note that the columns are separated by a single space.

Table 4: SAS data set structure.

```
   Data Set Name:   MYDIR.ENVIRONM              Type:
   Observations:    1042                        Record Len: 130
   Variables:       20
   Label:

             -----Alphabetic List of Variables and Attributes-----

  #  Variable    Type   Len  Pos  Format  Label
 19  BAND        Num      8  121  3.
  1  ID          Char     6    4
  7  IRREG       Char     1   32
  6  LAMELLA     Char     1   31
  5  LAUNCH      Char     1   30
  2  OUTCOME     Num      8   10  2.
 11  PHI1        Num      8   57  4.2
 13  PHI2        Num      8   73  4.2
  9  PHISPECK    Num      8   41  4.2
 20  RECERROR    Char     1  129
 10  RHO1        Num      8   49  3.
 12  RHO2        Num      8   65  3.
  8  RHOSPECK    Num      8   33  3.
 14  ROUND1      Num      8   81  3.
 15  ROUND2      Num      8   89  3.
 16  ROUND3      Num      8   97  3.
 17  ROUND4      Num      8  105  3.
 18  ROUND5      Num      8  113  3.
  4  SETUP       Char     4   26
  3  TEMP        Num      8   18  4.1
```

Table 5: ASCII file structure.

column	variable	positions	decimals
1	t	8	2
2	R	8	3
3	φ	8	3

8 Literature

Dalziel, S.B., 1992, *DigImage Particle Tracking,* Cambridge Environmental Research Consultants Ltd., University of Cambridge.

Dalziel, S.B., 1992, *DigImage System Overview,* Cambridge Environmental Research Consultants Ltd., University of Cambridge.

De Vos, J.C., Van der Genugten, B.B., and Minnaert, W., 1990, *Statistiek met SAS,* Academic Service, Schoonhoven.

SAS Institute, 1987, *SAS Guide to Macro Processing,* Version 6 Edition, SAS Institute, Cary.

SAS Institute, 1987, *SAS/GRAPH Guide for Personal Computers,* Version 6 Edition, SAS Institute, Cary.

SAS Institute, 1987, *SAS/STAT Guide for Personal Computers,* Version 6 Edition, SAS Institute, Cary.

Schwidefsky, K., and Ackermann, F., 1976, *Photogrammetrie: Grundlagen, Verfahren, Anwendungen,* Teubner, Stuttgart.

Van der Genugten, B.B., and Borm, P.E.M., 1991, *Het Onderscheiden van Kansspelen en Behendigheidsspelen met als Toepassing "Golden Ten",* Internal report Barents, Gassile & Mout, 's Gravenhage.

A Tracking parameters

```
                Base output file name: t10b03
                     Experiment title: Tape 10, Ball 3
                  Total tracking time:  1830.000000
      Spacing between acquired images:           2
Experimental time at start of tracking:      .000000
              Top of tracking window:          18
           Bottom of tracking window:         496
             Left of tracking window:         113
            Right of tracking window:         441
           Lower particle size limit:        -100
           Upper particle size limit:         300
           Minimum horizontal extent:          11
               Minimum vertical size:          16
     Lower particle location threshold:        96
     Upper particle location threshold:       128
                Minimum ellipticity:     1.000000
                Maximum ellipticity:     1.000000
           Maximum centroid mismatch:     1.000000
                          Lost cost:    60.000000
                     Pricing policy: 1
          Previous velocity weighting:     .500000
          Premium for small particles:    1.000000
          Premium for large particles:    1.000000
     Premium for elliptical particles:    1.000000
          Premium for faint particles:    1.000000
   Expected x velocity for new parts.:     .000000
   Expected y velocity for new parts.:     .000000
    Max velocity error for new parts.:  1000.000000
Ratio of y to x velocity error for new p:    1.000000
       Max rms error in reference map:   -2.000000
                      Centroid type: A
                  Particle polarity: G
               Rewind in background: F
         Type of background removal: N
                Time for background:    10.000000
     Type of ALU operation for removal:        15
    Result table for background removal:        0
        Type of background recording: N
            Display paths/cost etc.: M
            Display paths plot type: L
     Buffer containing particle paths:          0
              Paths intensity change:          6
                     Type of filter: O
```

B Transformation program

```
/* ********************************************************** */
/* THIS IS THE SAS PROGRAMME E:\MYSAS\G10\DIGTODAT.SAS.       */
/* IT READS DIGIMAGE FILES, CORRECTS THE TIME CODE,           */
/* SHIFTS THE IMAGE, SPLITS OFF AND TRANSFORMS TRAJECTORIES,  */
/* WRITES THE TRAJECTORIES TO ASCII FILES, AND PLOTS THEM.    */
/* ********************************************************** */

*  DETERMINE THE FILE NAMES  ;
   DM 'LOG; CLEAR; OUTPUT; CLEAR; PGM';
%WINDOW INFO COLOR=RED IROW=8 ICOLUMN=1 ROWS=7 COLUMNS=78
   #1 @1 'DigImage name     : ' INNAME 40 COLOR=YELLOW REQUIRED=YES
     @60 '(Without extension)'
   #3 @1 'Exp. nr. correct?: ' YN 1 COLOR=YELLOW REQUIRED=YES
     @60 '(Y/N)'
   #5 @1 'Time step         : 0.' STEP 2 COLOR=YELLOW REQUIRED=YES
     @60 '(seconds)';
%DISPLAY INFO;
   %LET NR1=%SUBSTR(&INNAME,%LENGTH(&INNAME)-1,1);
   %LET NR2=%SUBSTR(&INNAME,%LENGTH(&INNAME),1);
   %LET TAPE=%SUBSTR(&INNAME,%LENGTH(&INNAME)-4,2);
   %LET DIR=.\;
%WINDOW EXPNR COLOR=RED IROW=12 ICOLUMN=1 ROWS=3 COLUMNS=78
   #1 @1 "Exp. number: T&TAPE.B" NR 2 COLOR=WHITE REQUIRED=YES;
%MACRO NAMES;
   %IF (&YN=n OR &YN=N) %THEN %DO;
      %DISPLAY EXPNR;
      %LET NR1=%SUBSTR(&NR,1,1);
      %LET NR2=%SUBSTR(&NR,2,1);
   %END;
   %IF %LENGTH(&INNAME)>6 %THEN
        %LET DIR=%SUBSTR(&INNAME,1,%LENGTH(&INNAME)-6);
%MEND NAMES;
   %NAMES;
*  READ IND FILE  ;
DATA INDEX;
   INFILE "&INNAME..IND" FIRSTOBS=2 END=LAST;
   RETAIN T 0;
   IF _N_ NE 1 THEN T=T+&STEP;
   INPUT SAMPLE $ START END RMS N BUFFER;
   RECORD=START; OUTPUT;
   IF START NE END THEN DO; RECORD=END; OUTPUT; END;
   IF LAST THEN CALL SYMPUT('NUMBER',MAX(START,END));
   KEEP T RECORD BUFFER;
RUN;
PROC SORT DATA=INDEX;
   BY RECORD;
RUN;
*  DETERMINE THE COORDINATE SYSTEM  ;
   %LET TOP=18;
   %LET BOTTOM=496;
   %LET LEFT=113;
   %LET RIGHT=441;
   %LET XRANGE=%EVAL(&RIGHT-&LEFT);
   %LET YRANGE=%EVAL(&BOTTOM-&TOP);
DATA _NULL_;
   INFILE "&INNAME..WLD" RECFM=N;
   DO I=1 TO 3;
      INPUT BYTE PIB2.;
   END;
   CALL SYMPUT('RCODE',BYTE);
   STOP;
RUN;
```

```
%MACRO REFLECT;
   %IF &RCODE=0 %THEN %LET TOP=%EVAL(511-&BOTTOM);
   %ELSE %DO;
       %LET YRANGE=%EVAL(-&YRANGE);
       %LET TOP=%EVAL(511-&TOP);
   %END;
%MEND REFLECT;
   %REFLECT;
*  READ PRT FILE  ;
DATA POSITION;
   INFILE "&INNAME..PRT" RECFM=N;
   DO RECORD=1 TO &NUMBER;
      DO I=1 TO 3;
         INPUT BYTE PIB2.;
         IF I=2 THEN XDIG=1.447*(BYTE*&XRANGE/65535+&LEFT-255.5);
         ELSE IF I=3 THEN YDIG=BYTE*&YRANGE/65535+&TOP-255.5;
      END;
      OUTPUT;
   END;
   STOP;
   KEEP RECORD XDIG YDIG;
RUN;
*  DISTINGUISH THE TWO BALLS  ;
DATA BALL;
   MERGE INDEX POSITION;
   BY RECORD;
   IF (XDIG-30.85)**2+(YDIG-1.72)**2>50 THEN OUTPUT;
   DROP RECORD;
RUN;
PROC DATASETS LIBRARY=WORK;
   DELETE INDEX POSITION;
QUIT;
PROC SORT DATA=BALL;
   BY T;
RUN;
*  CORRECT THE TIME CODE  ;
   %LET PI= 3.14159265358979;
   %LET TWOPI=6.28318530717958;
   %LET LAGS=%STR(
   LF=LAG(F);
   IF LF<-3 AND F>0 THEN LF=LF+&TWOPI; );
%MACRO TIME;
   %IF &STEP=4 %THEN %LET LAGS=&LAGS%STR(
       F4=  4*F-3*LF;
       F3= (7*F-5*LF)/2;
       F2=  3*F-2*LF;
       F1= (5*F-3*LF)/2;
       F0=  2*F-  LF;
       F_1=(3*F-  LF)/2;
       F_2=    F;
       F_3=  (F+  LF)/2;
       F_4= LAG1(F);
       F_5=(LAG1(F)+LAG2(F))/2;
       F_6= LAG2(F);
       F_7=(LAG2(F)+LAG3(F))/2;
       F_8= LAG3(F); );
   %ELSE %IF &STEP=8 %THEN %LET LAGS=&LAGS%STR(
       F4=  3*F-2*LF;
       F3=(11*F-7*LF)/4;
       F2= (5*F-6*LF)/2;
       F1= (9*F-5*LF)/4;
       F0=  2*F-  LF;
       F_1=(7*F-3*LF)/4;
       F_2=(3*F-  LF)/2;
       F_3=(5*F-  LF)/4;
       F_4=    F;
       F_5=(3*F+  LF)/4;
```

```
        F_6=(   F+   LF)/2;
        F_7=(   F+3*LF)/4;
        F_8=         LF; );
    %ELSE %LET LAGS=&LAGS%STR(
        F4=   (8*F-5*LF)/3;
        F3=  (15*F-9*LF)/6;
        F2=   (7*F-4*LF)/3;
        F1=  (13*F-7*LF)/6;
        F0=    2*F-  LF;
        F_1=(11*F-5*LF)/6;
        F_2=  (5*F-2*LF)/3;
        F_3=  (9*F-3*LF)/6;
        F_4=  (4*F-  LF)/3;
        F_5=  (7*F-  LF)/6;
        F_6=     F;
        F_7=  (5*F+  LF)/6;
        F_8=  (2*F+  LF)/3; );
%MEND TIME;
    %TIME;
*   AND COUNT THE NUMBER OF TRAJECTORIES   ;
DATA BALL;
    SET BALL END=LAST;
    ARRAY FF F4 F3 F2 F1 F0 F_1-F_8;
    RETAIN M 1 IMAGE FLAGBUF DT 0 F R0;
    IMAGE=IMAGE+1;
    FDIG=ATAN((YDIG-1.72)/(XDIG-30.85));
    IF XDIG LE 30.85 THEN FDIG=FDIG-&PI;
    RDIG=SQRT((XDIG-30.85)**2+(YDIG-1.72)**2);
    &LAGS;
    IF BUFFER LT LAG(BUFFER) AND IMAGE GT 4 THEN DO;
        DIST=&PI-ABS(MOD(ABS(FDIG-F0),&TWOPI)-&PI);
        IF &PI-ABS(MOD(ABS(FDIG- F1),&TWOPI)-&PI) LT DIST OR
           &PI-ABS(MOD(ABS(FDIG-F_1),&TWOPI)-&PI) LT DIST THEN DO;
           XDIG=30.85+R0*COS(F0);
           YDIG= 1.72+R0*SIN(F0);
           FDIG=ATAN((YDIG-1.72)/(XDIG-30.85));
           IF XDIG LE 30.85 THEN FDIG=FDIG-&PI;
           RDIG=SQRT((XDIG-30.85)**2+(YDIG-1.72)**2);
           FLAGCOR=1;
        END;
        FLAGBUF=1;
    END;
    ELSE DO;
        IF FLAGBUF=1 AND IMAGE GT 5 THEN DO;
           MIN=&PI;
           DO I=1 TO 13;
              DIST=&PI-ABS(MOD(ABS(FDIG-FF{I}),&TWOPI)-&PI);
              IF DIST<MIN THEN DO; INDEX=I; MIN=DIST; END;
           END;
           DT=DT-2*(INDEX-5);
        END;
        FLAGBUF=0;
    END;
    T=T+DT;
    F=FDIG; R0=RDIG;
    PX=-66.868288+2.091377*XDIG-0.002287*YDIG;
    PY= -0.093121+0.001293*XDIG+2.090268*YDIG;
    PRHO=SQRT(PX*PX+PY*PY);
    IF PRHO-LAG(PRHO)>250 THEN DO;
       M=M+1;
       IMAGE=0;
    END;
    _TYPE_='FINAL';
    IF LAST THEN CALL SYMPUT('FILES',M);
    IF FLAGCOR NE 1 AND IMAGE GT 3 THEN OUTPUT;
    KEEP T XDIG YDIG _TYPE_;
RUN;
```

```
PROC SORT DATA=BALL NODUPKEY;
   BY T;
RUN;
*  ADJUST DEFAULT SYSTEM OPTIONS  ;
   OPTIONS NONUMBER PS=63 LS=78;
   GOPTIONS DEVICE=HPLJS2;
   AXIS2 ORDER=(100 TO 500 BY 100) LABEL=('R');
   AXIS3 ORDER=(1 TO 2 BY 0.1) LABEL=(F=CGREEK 'Df/D' F=SIMPLEX 't');
   SYMBOL1 V=NONE I=JOIN;
*  SPLIT OFF TRAJECTORIES  ;
   %LET FIRST=1;
%MACRO WRITE;
   %DO I=1 %TO &FILES;
   *  FIND THE SHIFT  ;
      %LET NO1=&FIRST;
      DATA CIRCLE;
         SET BALL (FIRSTOBS=&FIRST) END=LAST;
         RETAIN N 0;
         X1=-66.868288+2.091377*XDIG-0.002287*YDIG;
         Y1= -0.093121+0.001293*XDIG+2.090268*YDIG;
         PHI=ATAN(Y1/X1);
         IF X1<0 THEN PHI=PHI-&PI;
         IF (PHI-LAG(PHI)> 3) THEN N=N+1;
         IF (PHI-LAG(PHI)<-3) AND (_N_ NE 1) THEN N=N-1;
         IF N=1 THEN OUTPUT;
         RHO=SQRT(X1*X1+Y1*Y1);
         IF RHO-LAG(RHO)>250 OR LAST THEN DO;
            CALL SYMPUT('FIRST',_N_+&FIRST-1);
            %IF &FIRST>1 %THEN %DO;
                %IF &NR2=9 %THEN %DO;
                    %LET NR1=%EVAL(&NR1+1);
                    %LET NR2=0;
                %END;
                %ELSE %LET NR2=%EVAL(&NR2+1);
            %END;
            STOP;
         END;
         KEEP XDIG YDIG;
      RUN;
      PROC NLIN DATA=CIRCLE OUTEST=B;
         PARMS XS=0
               YS=0;
         A11= 1.0032119404E+00;
         A12= 1.3562415386E-03;
         A21= 4.3645268283E-03;
         A22= 9.9678761234E-01;
         A31=-4.6472509465E-02;
         A32= 8.8859632522E-02;
         A1= -8.2386070451E+01;
         A2=  1.4580318470E+02;
         A3= -1.8025764000E+03;
         X0 = 1.0559229131E+02;
         Y0 =-3.0562048483E+02;
         Z0 = 3.7882919356E+03;
         Z  = 470/12;
         CONST=220900-X0*X0-Y0*Y0;
         DZ=Z-Z0;
         N =A31*(XDIG-XS)+A32*(YDIG-YS)+A3;
         TX=A11*(XDIG-XS)+A12*(YDIG-YS)+A1;
         TY=A21*(XDIG-XS)+A22*(YDIG-YS)+A2;
         T =X0*TX+Y0*TY;
         T2=TX*TX+TY*TY;
         MODEL CONST=(DZ/N)*(2*T+(DZ*T2/N));
         DER.XS=(DZ/N)*((2*A31*T)/N-2*(A11*X0+A21*Y0)+
                        (2*DZ*A31*T2)/N**2-(2*DZ/N)*(A11*TX+A21*TY));
         DER.YS=(DZ/N)*((2*A32*T)/N-2*(A12*X0+A22*Y0)+
                        (2*DZ*A32*T2)/N**2-(2*DZ/N)*(A12*TX+A22*TY));
```

```
   RUN;
      DM 'OUTPUT; CLEAR; PGM';
*  KEEP THE SHIFT  ;
      %LET SHFTNAME=&DIR.SHIFT&TAPE;
      %LET OUTNAME=%SUBSTR(&INNAME,1,%LENGTH(&INNAME)-2)&NR1&NR2;
   DATA B;
    SET B (KEEP=_TYPE_ XS YS);
    FILE "&SHFTNAME..PAR" MOD;
    IF _TYPE_='FINAL' THEN DO;
      PUT "%SUBSTR(&OUTNAME,%LENGTH(&INNAME)-5) " (XS YS) (13.10 +1);
      OUTPUT;
    END;
   RUN;
*  CREATE DAT FILE  ;
   %IF &I=&FILES %THEN %LET NO2=&FIRST;
                  %ELSE %LET NO2=%EVAL(&FIRST-1);
   DATA BALL&I;
      MERGE BALL
            (KEEP=T XDIG YDIG _TYPE_ FIRSTOBS=&NO1 OBS=&NO2)
             B END=LAST;
      BY _TYPE_;
      FILE "&OUTNAME..DAT";
      RETAIN N T0 0;
      IF _N_=1 THEN T0=T;
      T=(T-T0)/100;
      XDIG=XDIG-XS-0.0234904199;
      YDIG=YDIG-YS+0.1997646069;
      A11= 1.0032119404E+00;
      A12= 1.3562415386E-03;
      A21= 4.3645268283E-03;
      A22= 9.9678761234E-01;
      A31=-4.6472509465E-02;
      A32= 8.8859632522E-02;
      A1= -8.2386070451E+01;
      A2=  1.4580318470E+02;
      A3= -1.8025764000E+03;
      X0 = 1.0559229131E+02;
      Y0 =-3.0562048483E+02;
      Z0 = 3.7882919356E+03;
      TX=A11*XDIG+A12*YDIG+A1;
      TY=A21*XDIG+A22*YDIG+A2;
      NZ=A31*XDIG+A32*YDIG+A3;
      ALFA1=X0-TX*Z0/NZ;
      ALFA2=TX/NZ;
      BETA1=Y0-TY*Z0/NZ;
      BETA2=TY/NZ;
      A=BETA2*BETA2+ALFA2*ALFA2-144;
      B=2*ALFA1*ALFA2*BETA2-2*ALFA2*ALFA2*BETA1+288*BETA1;
      C=ALFA1*ALFA1*BETA2*BETA2-2*ALFA1*ALFA2*BETA1*BETA2+
        ALFA2*ALFA2*BETA1*BETA1-144*BETA1*BETA1;
      PY=(-B+SQRT(B*B-4*A*C))/(2*A);
      IF (PY-BETA1)/BETA2 < 0 THEN PY=PY-SQRT(B*B-4*A*C)/A;
      PX=ALFA2*PY/BETA2+ALFA1-ALFA2*BETA1/BETA2;
      PRHO=SQRT(PX*PX+PY*PY);
      PPHI=ATAN(PY/PX);
      IF PX<0 THEN PPHI=PPHI-&PI;
      IF (PPHI-LAG(PPHI)> 3) THEN N=N+1;
      ELSE IF (PPHI-LAG(PPHI)<-3) AND (_N_ NE 1) THEN N=N-1;
      PHI_TOT=-PPHI+N*&TWOPI;
      PUT T 8.2 +1 PRHO 8.3 +1 PHI_TOT 8.3;
      IF PHI_TOT GE 0 THEN OUTPUT;
      IF LAST THEN CALL SYMPUT ('PHIMAX',10*FLOOR(PHI_TOT/10+1));
      PHI_DOT=(PHI_TOT-LAG(PHI_TOT))/(T-LAG(T));
      KEEP T PRHO PHI_TOT PHI_DOT;
   RUN;
*  PLOT THE TRAJECTORY  ;
      AXIS1 ORDER=(0 TO &PHIMAX BY 10) LABEL=('Phi');
```

```
      PROC GPLOT DATA=BALL&I;
         PLOT PRHO*PHI_TOT /GRID HAXIS=AXIS1 VAXIS=AXIS2;
         FOOTNOTE J=R "%SUBSTR(&OUTNAME,%LENGTH(&OUTNAME)-5)";
      RUN;
      PROC GPLOT DATA=BALL&I;
         PLOT PHI_DOT*PHI_TOT /GRID HAXIS=AXIS1 VAXIS=AXIS3;
      RUN;
   *  DELETE BALL#I  ;
      PROC DATASETS LIBRARY=WORK;
         DELETE BALL&I;
      QUIT;
   %END;
%MEND WRITE;
   %WRITE;
   FOOTNOTE '';
*  DELETE TEMPORARY DATA SETS  ;
PROC DATASETS LIBRARY=WORK;
   DELETE CIRCLE B;
RUN;
*  SOUND THE SIREN  ;
DATA _NULL_;
   DO I=0 TO 12.5664 BY .062832;
      CALL SOUND(3000-2000*COS(I),55);
   END;
RUN;

/* END OF PROGRAMME */
```

C Environmental data

-- TAPE=01 --

ID	OUTCOME	TEMP	SETUP	LAUNCH	LAMELLA	IRREG	RHOSPECK	PHISPECK	RHO1	PHI1	RHO2	PHI2	ROUND1	ROUND2	ROUND3	ROUND4	ROUND5	BAND	RECERROR
T01B01	24	27.0	1, 2																
T01B02	16	27.4							338	5.76									
T01B03	14	28.5				4			338	5.76									
T01B04	19	28.9																	
T01B05	9	28.9																	
T01B06	5	29.8																	
T01B07	17	29.1																470	
T01B08	18	29.4				3							258						
T01B09	16	29.1							292	5.24									
T01B10	16	29.6																	
T01B11	25	28.8																	
T01B12	9	29.8																	
T01B13	17	30.0																	
T01B14	8	29.2																271	
T01B15	24	30.4																	
T01B16	17	29.5																258	
T01B17	14	29.8																232	
T01B18	10	26.0	1, 3																
T01B19	14	28.8																	
T01B20	22	29.2											470					258	
T01B21	26	29.4											232						
T01B22	15	30.1			3														
T01B23	7	29.5							232	5.50			404						
T01B24	3	30.1																	
T01B25	7	29.9																	
T01B26	1	30.6																	
T01B27	14	30.5																	3
T01B28	26	30.2																	
T01B29	18	29.8																	
T01B30	10	30.2																271	
T01B31	25	30.6																	
T01B32	16	30.5																	
T01B33	16	30.6																	
T01B34	8	29.7																	
T01B35	6	31.2							292	5.50									
T01B36	2	30.4																	
T01B37	25	31.4																	
T01B38	6	30.2																	
T01B39	7	31.0																	
T01B40	3	29.1											238						
T01B41	10	26.8																	
T01B42	2	30.3																	
T01B43	19	30.7																	
T01B44	25	30.9																	
T01B45	1	30.4																	

-- TAPE=01 --

ID	OUTCOME	TEMP	SETUP	LAUNCH	LAMELLA	IRREG	RHOSPECK	PHISPECK	RHO1	PHI1	RHO2	PHI2	ROUND1	ROUND2	ROUND3	ROUND4	ROUND5	BAND	RECERROR
T01B46	22	31.0																	
T01B47	20	30.4																238	
T01B48	22	30.6																	
T01B49	1	30.8											271						
T01B50	20	31.0																	
T01B51	23	30.6																	
T01B52	6	31.1											271						
T01B53	23	31.7																	
T01B54	3	30.5																	
T01B55	12	30.7																	
T01B56	2	31.2																	
T01B57	10	31.5											338						
T01B58	19	31.8																	
T01B59	25	30.8																	
T01B60	11	31.9											238						
T01B61	1	31.7																238	
T01B62	26	31.9			1														
T01B63	1	30.8																	
T01B64	16	30.8																	
T01B65	10	31.1																	
T01B66	9	31.6																	
T01B67	15	32.0																	
T01B68	5	30.1																	
T01B69	20	31.0																	
T01B70	10	30.9																	
T01B71	19	32.0																	
T01B72	17	31.1																	
T01B73	20	31.9			3														
T01B74	3	31.4																	
T01B75	17	31.6				6			470	1.05	292	3.93							
T01B76	1	31.6											338	271	205				
T01B77	10	31.7																	
T01B78	18	31.5																	
T01B79	13	31.4																	
T01B80	14	31.3																	

-- TAPE=02 --

ID	OUTCOME	TEMP	SETUP	LAUNCH	LAMELLA	IRREG	RHOSPECK	PHISPECK	RHO1	PHI1	RHO2	PHI2	ROUND1	ROUND2	ROUND3	ROUND4	ROUND5	BAND	RECERROR
T02B01	4	27.2	1, 3										205						
T02B02	24	30.1							338	1.57			404						
T02B03	11	31.0							338	3.14									
T02B04	18	31.6																	
T02B05	3	31.4			2								238						
T02B06	20	32.1				4			338	1.05			238						
T02B07	12	31.6																271	
T02B08	20	32.2							383	1.57									
T02B09	14	31.3				4	470	0.00											
T02B10	11	31.5																	
T02B11	12	31.8																232	
T02B12	6	32.0																	
T02B13	20	32.0				4	292	0.00	292	0.00									
T02B14	26	31.1																	
T02B15	15	31.0																	
T02B16	6	31.6																	
T02B17	9	31.8																	
T02B18	9	32.2																	
T02B19	13	30.4																	
T02B20	16	32.0			2														
T02B21	12	31.6			2														
T02B22	23	32.4																	
T02B23	10	32.2			2														
T02B24	22	32.5																	
T02B25	21	31.7																	
T02B26	9	27.6											238						
T02B27	16	31.4			3								470						
T02B28	21	31.5			3														
T02B29	16	31.2																	
T02B30	2	31.7																	
T02B31	22	31.8											238						
T02B32	12	32.4																	
T02B33	20	32.5											238						
T02B34	6	32.4																	
T02B35	3	32.2																	
T02B36	17	31.7																	
T02B37	20	32.4																	
T02B38	25	31.9																	
T02B39	26	31.4			2														
T02B40	9	32.0																	
T02B41	2	32.6																	
T02B42	13	32.5																	
T02B43	15	32.4																	
T02B44	10	32.3											238						
T02B45	22	32.1																	

-- TAPE=02 --

ID	OUTCOME	TEMP	SETUP	LAUNCH	LAMELLA	IRREG	RHOSPECK	PHISPECK	RHO1	PHI1	RHO2	PHI2	ROUND1	ROUND2	ROUND3	ROUND4	ROUND5	BAND	RECERROR
T02B46	15	31.6																	
T02B47	1	31.6																	
T02B48	6	32.0																	
T02B49	4	32.2																	
T02B50	8	31.7																	
T02B51	8	31.8																	3
T02B52	12	32.0																	
T02B53	25	32.0																	

-- TAPE=03 --

ID	OUTCOME	TEMP	SETUP	LAUNCH	LAMELLA	IRREG	RHOSPECK	PHISPECK	RHO1	PHI1	RHO2	PHI2	ROUND1	ROUND2	ROUND3	ROUND4	ROUND5	BAND	RECERROR
T03B01	13	27.7																	
T03B02	18	29.0																	
T03B03	23	29.0																271	
T03B04	10	28.8			3													271	
T03B05	3	29.2																	
T03B06	22	29.8																	
T03B07	10	29.5											271						
T03B08	10	30.6				3													
T03B09	4	30.2			3														
T03B10	24	30.3																	
T03B11	15	29.8																	
T03B12	11	30.8																	
T03B13	5	29.9																	
T03B14	3	30.4							470	3.14			232						
T03B15	20	30.1																	
T03B16	24	29.9																	
T03B17	23	30.5											271						
T03B18	26	31.0																292	
T03B19	22	31.4																	
T03B20	17	31.0																	
T03B21	12	30.9																	
T03B22	18	31.2																271	
T03B23	6	30.8																	
T03B24	13	31.4																	
T03B25	22	31.1																	
T03B26	21	31.1																	
T03B27	26	30.3			2														
T03B28	9	30.9																	
T03B29	5	31.1																	
T03B30	21	31.6																	
T03B31	4	31.1			2														
T03B32	13	31.9																	
T03B33	11	31.4																	
T03B34	6	31.5																	
T03B35	5	26.4							258	1.57									
T03B36	1	29.9																	
T03B37	18	31.1																	
T03B38	8	31.0											258						
T03B39	12	32.1		3														238	
T03B40	2	30.8																	
T03B41	21	31.0																	
T03B42	21	31.3																	
T03B43	25	31.3																	
T03B44	4	32.4																	
T03B45	24	32.2																	

-- TAPE=03 --

ID	OUTCOME	TEMP	SETUP	LAUNCH	LAMELLA	IRREG	RHOSPECK	PHISPECK	RHO1	PHI1	RHO2	PHI2	ROUND1	ROUND2	ROUND3	ROUND4	ROUND5	BAND	RECERROR
T03B46	18	31.8				4	383	5.24											
T03B47	5	33.0																	
T03B48	13	31.2																	
T03B49	18	31.2																	
T03B50	1	31.6																	
T03B51	9	32.2																	
T03B52	9	32.5																	
T03B53	17	32.3																	
T03B54	16	32.8																	
T03B55	1	32.4																	
T03B56	20	31.9			3														
T03B57	15	31.7																	
T03B58	2	32.6																	
T03B59	16	32.2																	
T03B60	16	32.7																	
T03B61	14	32.0			3														
T03B62	9	33.0											238						
T03B63	12	32.3																	
T03B64	5	33.2											238						
T03B65	5	33.0		4	2														
T03B66	14	32.7																	
T03B67	11	32.0																	
T03B68	9	33.4																	
T03B69	25	32.5																	

-- TAPE=04 --

ID	OUTCOME	TEMP	SETUP	LAUNCH	LAMELLA	IRREG	RHOSPECK	PHISPECK	RHO1	PHI1	RHO2	PHI2	ROUND1	ROUND2	ROUND3	ROUND4	ROUND5	BAND	RECERROR
T04B01	13	30.7	1, 2																
T04B02	8	32.5																	
T04B03	13	32.3																	
T04B04	25	32.8																	
T04B05	5	33.4			3														
T04B06	15	33.4																	
T04B07	18	32.9																	
T04B08	9	32.8																	
T04B09	22	33.8																	
T04B10	4	33.1																	
T04B11	18	34.1																	
T04B12	10	32.9																	
T04B13	12	33.4																	
T04B14	16	33.6																	
T04B15	15	33.7											271	238					
T04B16	22	32.9																	
T04B17	14	33.4																	
T04B18	16	33.4																	
T04B19	18	33.3																	
T04B20	4	33.2																	
T04B21	20	33.4																	
T04B22	15	33.2			3								470	258					
T04B23	25	32.9											258	205					
T04B24	19	32.9											258					238	
T04B25	25	33.2																	
T04B26	16	33.3																	
T04B27	3	33.6																	
T04B28	6	33.6																271	
T04B29	18	33.6			3				271	5.24									
T04B30	2	33.1																	
T04B31	15	34.6							238	5.24									
T04B32	24	34.0																	
T04B33	14	33.5																	
T04B34	19	32.9							232	5.06									
T04B35	17	32.3																	
T04B36	8	30.9																	
T04B37	19	31.5			3														2
T04B38	18	32.7																	
T04B39	16	31.8																	3
T04B40	5	31.6																	
T04B41	6	34.2																	
T04B42	26	34.0																	
T04B43	7	32.7																	
T04B44	18	34.1																	
T04B45	17	33.7																	

-- TAPE=04 --

ID	OUTCOME	TEMP	SETUP	LAUNCH	LAMELLA	IRREG	RHOSPECK	PHISPECK	RHO1	PHI1	RHO2	PHI2	ROUND1	ROUND2	ROUND3	ROUND4	ROUND5	BAND	RECERROR
T04B46	17	33.6																	
T04B47	22	33.2																	
T04B48	25	32.8																	
T04B49	14	34.0											205						
T04B50	26	33.9																	
T04B51	21	33.4				5													
T04B52	13	33.4											258						
T04B53	20	34.0																258	
T04B54	5	32.4											271						
T04B55	2	34.0																	
T04B56	20	33.7																	
T04B57	6	32.7																	
T04B58	12	34.4																	
T04B59	11	34.6				5													
T04B60	12	34.1																	
T04B61	9	33.5				4							205						
T04B62	4	33.5																232	
T04B63	23	34.3																	
T04B64	13	32.5																	
T04B65	21	33.7																	
T04B66	1	32.7																	
T04B67	6	33.8																	
T04B68	16	34.6			3														
T04B69	5	33.6																	
T04B70	20	34.1							383	4.71									
T04B71	8	31.9																	
T04B72	15	34.1																	

-- TAPE=05 --

ID	OUTCOME	TEMP	SETUP	LAUNCH	LAMELLA	IRREG	RHOSPECK	PHISPECK	RHO1	PHI1	RHO2	PHI2	ROUND1	ROUND2	ROUND3	ROUND4	ROUND5	BAND	RECERROR
T05B01	12	27.9	1, 5																
T05B02	21	29.3																	
T05B03	18	29.6																238	
T05B04	5	29.5																	
T05B05	18	30.7																258	
T05B06	25	30.3																	
T05B07	18	30.7																	
T05B08	3	30.5																	
T05B09	19	31.2																	
T05B10	9	31.0																	
T05B11	21	30.4																	
T05B12	16	31.2																	
T05B13	25	30.8																	
T05B14	5	30.4																	
T05B15	11	30.8																	
T05B16	22	32.0																	
T05B17	4	31.2																	
T05B18	19	31.4																	
T05B19	21	31.1																	
T05B20	14	31.7		3															
T05B21	22	31.8																	
T05B22	18	30.4											338	292					
T05B23	6	31.4																	
T05B24	7	31.0																	
T05B25	18	32.8			3														
T05B26	20	30.7				3													
T05B27	8	30.6			2														
T05B28	21	32.8																	
T05B29	20	32.1																	
T05B30	6	31.1																	
T05B31	20	33.4																	
T05B32	2	32.2																	
T05B33	10	31.4																	
T05B34	9	32.9																	
T05B35	1	27.2																	
T05B36	7	31.4																	
T05B37	4	32.4																	
T05B38	4	32.8																	
T05B39	14	32.8							383	5.50									
T05B40	25	32.5																	
T05B41	14	30.9																	
T05B42	19	33.1																	
T05B43	12	33.2																	
T05B44	18	33.3																	
T05B45	22	33.0											338	292	238	232			

TAPE=05

ID	OUTCOME	TEMP	SETUP	LAUNCH	LAMELLA	IRREG	RHOSPECK	PHISPECK	RHO1	PHI1	RHO2	PHI2	ROUND1	ROUND2	ROUND3	ROUND4	ROUND5	BAND	RECERROR
T05B46	18	33.5																	
T05B47	1	32.8																	
T05B48	14	33.8																	
T05B49	18	33.6																	
T05B50	8	33.2																	
T05B51	14	33.8																	
T05B52	9	33.0																	
T05B53	10	33.8																	
T05B54	16	33.4																	
T05B55	23	33.6			2														
T05B56	12	33.6																	3
T05B57	14	33.9			3								338						
T05B58	8	33.8																	
T05B59	1	33.6																	
T05B60	9	34.0																	
T05B61	20	34.2																	
T05B62	1	33.8																	
T05B63	2	34.0																	
T05B64	20	33.6																	
T05B65	6	34.4																	
T05B66	17	34.5																	
T05B67	4	34.7																	

TAPE=06

ID	OUTCOME	TEMP	SETUP	LAUNCH	LAMELLA	IRREG	RHOSPECK	PHISPECK	RHO1	PHI1	RHO2	PHI2	ROUND1	ROUND2	ROUND3	ROUND4	ROUND5	BAND	RECERROR
T06B01	4	28.2																	
T06B02	26	32.0			3														
T06B03	13	33.1																	
T06B04	15	33.5																	
T06B05	18	33.1			2														
T06B06	2	33.3																	
T06B07	1	33.6																	
T06B08	2	33.3																	
T06B09	11	33.9																	
T06B10	12	33.6			3				271	2.36									
T06B11	23	33.7																	
T06B12	18	33.7																	
T06B13	3	32.7							258	2.36									
T06B14	15	34.3											258						
T06B15	14	34.1			2														
T06B16	12	34.2																	
T06B17	15	33.6																	
T06B18	22	33.9			3				238	1.75									
T06B19	25	34.2																	
T06B20	23	34.0			3														
T06B21	17	34.5																	
T06B22	8	33.3																	
T06B23	16	34.8																	
T06B24	7	33.4		3															
T06B25	15	34.3																	
T06B26	26	34.2							238	1.48									
T06B27	10	35.0																	
T06B28	6	35.1				5			205	0.00									
T06B29	14	34.4							205	0.00									
T06B30	22	33.6				1													
T06B31	11	34.2																	
T06B32	20	35.2																	
T06B33	18	34.2							232	1.05									
T06B34	13	34.5							205	5.76									
T06B35	18	32.2	1, 4																
T06B36	21	34.2																	
T06B37	11	34.3																	
T06B38	24	34.7			3														
T06B39	14	34.3																	
T06B40	5	34.8																	
T06B41	11	34.6																	
T06B42	11	35.0																	
T06B43	1	34.9			2														
T06B44	14	34.8			3				311	4.71									
T06B45	12	34.8																	

-- TAPE=06 --

ID	OUTCOME	TEMP	SETUP	LAUNCH	LAMELLA	IRREG	RHOSPECK	PHISPECK	RHO1	PHI1	RHO2	PHI2	ROUND1	ROUND2	ROUND3	ROUND4	ROUND5	BAND	RECERROR
T06B46	22	34.7																	
T06B47	1	34.3																	
T06B48	25	33.6																	
T06B49	1	35.0																	
T06B50	23	35.0																	
T06B51	3	34.5																	
T06B52	22	35.3																	
T06B53	11	34.7																	
T06B54	22	35.2			3														
T06B55	8	34.3																	
T06B56	14	35.2																	
T06B57	2	33.1																	
T06B58	12	35.5																	
T06B59	6	35.2																	
T06B60	2	34.8																	
T06B61	14	35.4																	
T06B62	19	34.6																	
T06B63	13	34.5																	3
T06B64	16	35.4																	
T06B65	18	35.0																	
T06B66	2	35.0			2														
T06B67	15	35.6																	3
T06B68	20	33.7																	
T06B69	20	34.6																	

---------- TAPE=07 ----------

ID	OUTCOME	TEMP	SETUP	LAUNCH	LAMELLA	IRREG	RHOSPECK	PHISPECK	RHO1	PHI1	RHO2	PHI2	ROUND1	ROUND2	ROUND3	ROUND4	ROUND5	BAND	RECERROR
T07B01	4	25.9																	
T07B02	1	29.0			3														
T07B03	12	29.9																	
T07B04	3	30.4							470	0.00									
T07B05	23	30.9											383						
T07B06	8	30.8																	
T07B07	24	31.2																	
T07B08	18	31.5																	
T07B09	18	31.3											338						
T07B10	10	31.2																	
T07B11	25	31.9																	
T07B12	14	32.0																	
T07B13	10	32.2																	
T07B14	5	31.8																	
T07B15	8	31.6																232	
T07B16	12	32.8																	
T07B17	1	32.1																	
T07B18	10	32.7																	
T07B19	22	32.8		1															
T07B20	3	32.5																	
T07B21	25	32.9																	
T07B22	20	32.8																	
T07B23	2	32.0																	
T07B24	9	31.5																	
T07B25	10	33.3																	
T07B26	12	33.2																	
T07B27	10	33.0			1														
T07B28	21	32.8																	
T07B29	22	32.8				4	292	5.50											
T07B30	16	32.6																	
T07B31	21	33.4																	
T07B32	2	33.0																	
T07B33	10	33.4																	
T07B34	18	32.3																	
T07B35	12	32.4																	
T07B36	26	30.4																	1
T07B37	2	32.1																	
T07B38	17	31.9																	
T07B39	9	33.0																	
T07B40	20	33.7																	
T07B41	18	32.4																	
T07B42	16	32.9																	1
T07B43	17	32.5																	
T07B44	11	33.4																	
T07B45	14	34.0																	

-- TAPE=07 --

ID	OUTCOME	TEMP	SETUP	LAUNCH	LAMELLA	IRREG	RHOSPECK	PHISPECK	RHO1	PHI1	RHO2	PHI2	ROUND1	ROUND2	ROUND3	ROUND4	ROUND5	BAND	RECERROR
T07B46	2	34.3																	
T07B47	15	34.1																	
T07B48	26	33.9			3														
T07B49	3	34.3																	
T07B50	25	34.1																	
T07B51	26	34.0																	
T07B52	9	34.5																	
T07B53	2	34.3																	
T07B54	2	34.7																	
T07B55	14	33.4																	
T07B56	15	32.6			3														
T07B57	12	34.6																	
T07B58	14	34.6																	
T07B59	17	34.5																	3
T07B60	22	34.0																	
T07B61	12	33.8																	
T07B62	13	34.2																	
T07B63	12	34.6																	
T07B64	24	33.8		1															
T07B65	13	34.7																	
T07B66	24	34.8																	
T07B67	7	35.0																	
T07B68	26	35.2																	

TAPE=08

ID	OUTCOME	TEMP	SETUP	LAUNCH	LAMELLA	IRREG	RHOSPECK	PHISPECK	RHO1	PHI1	RHO2	PHI2	ROUND1	ROUND2	ROUND3	ROUND4	ROUND5	BAND	RECERROR
T08B01	24	32.0																	
T08B02	3	33.5											292						
T08B03	2	33.9																	
T08B04	9	33.9																	
T08B05	21	33.5																292	
T08B06	6	33.7																	
T08B07	13	34.2																	
T08B08	13	34.0																	
T08B09	16	34.2			3														
T08B10	10	34.3																	
T08B11	8	34.4																	
T08B12	20	34.8																	
T08B13	16	34.0																	
T08B14	7	34.6																	
T08B15	6	34.8																	
T08B16	13	34.9																	
T08B17	16	34.5																	
T08B18	16	35.0																	
T08B19	25	34.2																338	
T08B20	14	34.5																	
T08B21	8	34.8											232						
T08B22	6	34.2																	
T08B23	6	34.6																	
T08B24	12	34.8																	
T08B25	14	34.3																	
T08B26	21	34.7																	
T08B27	7	33.4																	6
T08B28	23	33.6																	
T08B29	13	34.5																	
T08B30	7	34.9																	
T08B31	25	35.1																	
T08B32	16	34.6																	
T08B33	8	35.0																	
T08B34	15	33.9				6												271	
T08B35	20	31.7				5													
T08B36	15	33.6																	
T08B37	17	34.3																	
T08B38	1	33.1																	4
T08B39	3	34.2																	3
T08B40	6	34.6																	
T08B41	7	34.6																	
T08B42	23	34.9																	
T08B43	24	34.5																	
T08B44	5	34.6																	
T08B45	12	34.9																	6

-- TAPE=08 --

ID	OUTCOME	TEMP	SETUP	LAUNCH	LAMELLA	IRREG	RHOSPECK	PHISPECK	RHO1	PHI1	RHO2	PHI2	ROUND1	ROUND2	ROUND3	ROUND4	ROUND5	BAND	RECERROR
T08B46	24	33.0																	
T08B47	6	34.2																	
T08B48	21	35.4																	
T08B49	1	34.6											238						
T08B50	5	35.2																	
T08B51	11	34.2																	
T08B52	20	34.8																	
T08B53	20	34.8																	
T08B54	4	34.6																	6
T08B55	20	33.7																	
T08B56	15	35.0			3														
T08B57	23	35.4			3														
T08B58	16	34.4											271						
T08B59	9	35.2																	
T08B60	15	35.1																	
T08B61	12	35.1																	
T08B62	12	34.1																	
T08B63	11	34.8																	
T08B64	10	34.8																	
T08B65	23	34.0											292	271					
T08B66	10	34.1																	
T08B67	3	34.8																	
T08B68	21	34.7																	
T08B69	6	34.6																	
T08B70	26	35.2																	
T08B71	25	34.6																	

TAPE=09

ID	OUTCOME	TEMP	SETUP	LAUNCH	LAMELLA	IRREG	RHOSPECK	PHISPECK	RHO1	PHI1	RHO2	PHI2	ROUND1	ROUND2	ROUND3	ROUND4	ROUND5	BAND	RECERROR
T09B01	20	27.4																	6
T09B02	7	29.4																	2
T09B03	2	30.8																271	
T09B04	1	31.7																	
T09B05	14	31.9		1	3														
T09B06	13	32.0																	
T09B07	16	32.3																	
T09B08	11	32.5																	
T09B09	16	32.4																	
T09B10	23	32.6											444						
T09B11	8	32.0																	
T09B12	20	34.0																	
T09B13	11	32.8																	
T09B14	15	33.8																	
T09B15	4	33.4																	
T09B16	20	32.4																	
T09B17	21	32.2																	
T09B18	9	33.3																	
T09B19	2	33.6																	
T09B20	26	33.1																	
T09B21	12	33.6																	
T09B22	5	33.4																	
T09B23	1	33.8		1															
T09B24	13	32.6																	
T09B25	18	33.2																	
T09B26	11	33.3																	
T09B27	10	32.0																	
T09B28	16	34.0																	
T09B29	10	34.2																	
T09B30	25	34.2											258						
T09B31	11	34.3																	
T09B32	17	33.2			3														
T09B33	23	34.1				4	338	2.36											
T09B34	17	27.6																	6
T09B35	21	31.7		1															
T09B36	14	32.6																	
T09B37	6	32.8																	
T09B38	7	33.5			2														
T09B39	18	32.7			3														
T09B40	20	33.0																	
T09B41	14	33.0																271	
T09B42	16	33.9																	
T09B43	13	33.9																	
T09B44	15	34.2																	
T09B45	6	34.0																	

TAPE=09

ID	OUTCOME	TEMP	SETUP	LAUNCH	LAMELLA	IRREG	RHOSPECK	PHISPECK	RHO1	PHI1	RHO2	PHI2	ROUND1	ROUND2	ROUND3	ROUND4	ROUND5	BAND	RECERROR
T09B46	24	32.7																	
T09B47	8	33.9																	
T09B48	16	33.8																	
T09B49	14	34.1																	
T09B50	11	33.6																	
T09B51	6	34.0																	
T09B52	12	33.3																	
T09B53	14	33.4																	
T09B54	17	34.0			3														
T09B55	16	33.9			3														
T09B56	15	33.3																	
T09B57	1	33.5																	
T09B58	23	34.0																	
T09B59	15	33.7											232						
T09B60	18	34.5				4	404	5.93											
T09B61	13	33.0																	
T09B62	4	34.0																	
T09B63	21	33.1																	
T09B64	5	33.2		1															
T09B65	25	34.5																	
T09B66	24	34.3																	

-- TAPE=10 --

ID	OUTCOME	TEMP	SETUP	LAUNCH	LAMELLA	IRREG	RHOSPECK	PHISPECK	RHO1	PHI1	RHO2	PHI2	ROUND1	ROUND2	ROUND3	ROUND4	ROUND5	BAND	RECERROR
T10B01	7	31.0		1															
T10B02	18	32.8			3														
T10B03	17	33.0											338						
T10B04	24	32.9			2														
T10B05	17	33.4		1									292						
T10B06	2	33.5																	
T10B07	23	33.1		2															
T10B08	2	32.8											338					292	
T10B09	19	33.3																	
T10B10	13	33.4																	
T10B11	11	33.1																	
T10B12	12	33.5																	
T10B13	22	33.9																	
T10B14	19	33.6											338						
T10B15	3	33.5																271	
T10B16	16	32.9																	
T10B17	6	33.6																238	
T10B18	8	34.0																	
T10B19	20	33.9																	
T10B20	25	32.9																	
T10B21	20	32.8																	
T10B22	16	33.2																	
T10B23	6	33.8																	
T10B24	23	33.1			3														
T10B25	6	33.0																	
T10B26	2	33.7																	
T10B27	13	33.5																	
T10B28	11	33.9																	
T10B29	21	33.7																	3
T10B30	4	33.4																	
T10B31	25	34.0																	
T10B32	6	34.1																	
T10B33	1	33.7																	
T10B34	21	33.9																	
T10B35	16	33.7																	
T10B36	8	30.9																	
T10B37	19	32.8																	
T10B38	18	32.3																232	
T10B39	16	33.0																	
T10B40	8	33.3																	
T10B41	6	33.3																	
T10B42	8	33.4																	
T10B43	21	33.2																	
T10B44	19	32.8																238	
T10B45	5	32.8		2															

-- TAPE=10 --

ID	OUTCOME	TEMP	SETUP	LAUNCH	LAMELLA	IRREG	RHOSPECK	PHISPECK	RHO1	PHI1	RHO2	PHI2	ROUND1	ROUND2	ROUND3	ROUND4	ROUND5	BAND	RECERROR
T10B46	5	33.9																	3
T10B47	13	33.1																	
T10B48	4	32.9																	
T10B49	4	32.4																	
T10B50	10	33.4			3														
T10B51	9	33.8																	
T10B52	18	33.8																	
T10B53	19	33.0		2															
T10B54	7	32.5																	
T10B55	23	33.7											258						
T10B56	5	32.9																	
T10B57	16	33.3																	
T10B58	11	33.7																	
T10B59	12	32.4																	
T10B60	5	33.6																	
T10B61	1	33.7																	
T10B62	4	33.6			3														
T10B63	2	33.4																	
T10B64	11	33.6																	
T10B65	5	33.6			3														
T10B66	19	33.8																	
T10B67	10	33.5			3														
T10B68	7	34.0																	
T10B69	10	34.2																	
T10B70	18	33.5											238						
T10B71	18	33.0				5													
T10B72	26	32.9																	
T10B73	19	33.8											470	205					
T10B74	2	33.6																	

TAPE=11

ID	OUTCOME	TEMP	SETUP	LAUNCH	LAMELLA	IRREG	RHOSPECK	PHISPECK	RHO1	PHI1	RHO2	PHI2	ROUND1	ROUND2	ROUND3	ROUND4	ROUND5	BAND	RECERROR
T11B01	16	24.3																	
T11B02	26	27.7			3														
T11B03	16	29.6																	
T11B04	7	30.2																	
T11B05	21	30.6																	
T11B06	20	30.7																292	
T11B07	6	30.2																	
T11B08	11	31.0																	
T11B09	11	29.9																232	
T11B10	22	31.5																	
T11B11	6	30.2																	
T11B12	8	31.4																	
T11B13	22	31.7																	
T11B14	22	30.8																	
T11B15	9	31.2				5													
T11B16	6	31.5																	
T11B17	1	31.9																	
T11B18	3	31.5																	
T11B19	14	31.2			2													238	
T11B20	21	32.3											338						
T11B21	5	31.5																	
T11B22	19	31.9																	
T11B23	10	31.3																	
T11B24	22	32.2																	
T11B25	15	31.5																	
T11B26	18	31.3																	6
T11B27	9	32.4																	
T11B28	2	32.5		1															
T11B29	8	32.6																	
T11B30	22	32.9																	
T11B31	22	32.0																	
T11B32	13	32.4																	
T11B33	26	26.2		3															
T11B34	13	30.0																	
T11B35	26	31.2																	
T11B36	16	32.5			1														
T11B37	18	32.4																	2
T11B38	8	31.5																	
T11B39	18	32.9																	
T11B40	18	32.5																	
T11B41	8	31.7																	
T11B42	15	33.0																	
T11B43	21	33.2																	
T11B44	25	32.3																	
T11B45	13	33.2																	

TAPE=11

ID	OUTCOME	TEMP	SETUP	LAUNCH	LAMELLA	IRREG	RHOSPECK	PHISPECK	RHO1	PHI1	RHO2	PHI2	ROUND1	ROUND2	ROUND3	ROUND4	ROUND5	BAND	RECERROR
T11B46	24	33.1																	
T11B47	21	32.8			1														
T11B48	21	32.0																	
T11B49	12	32.5																	
T11B50	10	33.5																	
T11B51	21	32.9																	
T11B52	26	32.5																	
T11B53	10	33.3																	
T11B54	5	33.2																	
T11B55	11	32.6																	
T11B56	19	33.4																	
T11B57	8	32.8																	
T11B58	15	33.4		1															
T11B59	12	33.2																	
T11B60	17	33.3																	
T11B61	5	33.2																	
T11B62	10	31.8																	
T11B63	10	33.6																	
T11B64	7	32.9																	
T11B65	16	33.6		2															

-- TAPE=12 --

ID	OUTCOME	TEMP	SETUP	LAUNCH	LAMELLA	IRREG	RHOSPECK	PHISPECK	RHO1	PHI1	RHO2	PHI2	ROUND1	ROUND2	ROUND3	ROUND4	ROUND5	BAND	RECERROR
T12B01	11	30.3			1														
T12B02	10	32.3																	
T12B03	12	32.8																	
T12B04	22	32.7																	
T12B05	20	32.4											338						
T12B06	24	32.0											338						3
T12B07	15	32.2											470						
T12B08	9	32.7																	
T12B09	12	33.1		1															
T12B10	19	33.4																	
T12B11	13	33.0																	
T12B12	12	33.3																	
T12B13	15	33.3																238	
T12B14	21	33.3																	
T12B15	7	32.2																	
T12B16	16	33.5																	
T12B17	8	33.2																	
T12B18	17	33.3											205						
T12B19	20	33.3			3														
T12B20	12	32.5																	
T12B21	3	33.4																	
T12B22	7	33.3																	
T12B23	18	33.6																	
T12B24	18	32.8																	
T12B25	12	33.3																	
T12B26	17	35.1																	
T12B27	3	33.9																	
T12B28	13	34.1																	
T12B29	10	34.4																	
T12B30	8	34.1																	
T12B31	19	34.0		1															
T12B32	18	33.1																	
T12B33	22	33.6																	
T12B34	10	33.6																	
T12B35	21	31.3																	
T12B36	16	32.4																	
T12B37	11	32.9																	
T12B38	18	33.1																	
T12B39	5	33.4																	
T12B40	24	33.2			3														
T12B41	25	33.9																	
T12B42	11	33.6																	
T12B43	2	34.0		1															
T12B44	4	33.4																292	
T12B45	11	33.6											338						

TAPE=12

ID	OUTCOME	TEMP	SETUP	LAUNCH	LAMELLA	IRREG	RHOSPECK	PHISPECK	RHO1	PHI1	RHO2	PHI2	ROUND1	ROUND2	ROUND3	ROUND4	ROUND5	BAND	RECERROR
T12B46	4	33.5																	
T12B47	15	33.6																	
T12B48	14	33.0																	
T12B49	12	32.4																	
T12B50	9	34.0																	
T12B51	20	33.7																	
T12B52	6	32.9																	
T12B53	1	34.2											338						
T12B54	22	34.1		1									292	271					
T12B55	13	33.5		1															
T12B56	16	33.8																	
T12B57	21	34.1																	
T12B58	6	33.7																	
T12B59	17	33.0																	
T12B60	8	33.1																	
T12B61	14	34.1																	
T12B62	17	33.8											470						
T12B63	13	33.9			3														
T12B64	24	34.9		2	2														
T12B65	17	33.8																	
T12B66	23	33.8											338						
T12B67	20	34.1											258						
T12B68	7	33.9																	
T12B69	16	34.2		1															
T12B70	23	33.3		2															
T12B71	17	33.6																	

TAPE=13

ID	OUTCOME	TEMP	SETUP	LAUNCH	LAMELLA	IRREG	RHOSPECK	PHISPECK	RHO1	PHI1	RHO2	PHI2	ROUND1	ROUND2	ROUND3	ROUND4	ROUND5	BAND	RECERROR
T13B01	8	24.8																	
T13B02	3	28.6																	
T13B03	16	29.8																	
T13B04	10	30.2																	
T13B05	20	30.5											258						
T13B06	13	29.8																	
T13B07	22	30.5																	
T13B08	24	31.0																	
T13B09	20	30.8																	
T13B10	3	30.8																	
T13B11	4	31.5																	
T13B12	1	30.9																	
T13B13	15	32.0		1															
T13B14	15	31.6																	
T13B15	9	31.4																	
T13B16	12	31.9											271						
T13B17	11	31.9											338						
T13B18	20	31.8																	
T13B19	9	31.6																	
T13B20	1	32.0																	
T13B21	12	32.0																	
T13B22	6	32.2																	
T13B23	5	32.3																	
T13B24	13	32.4											470	205					
T13B25	15	32.2																	
T13B26	25	32.6																	
T13B27	5	31.8																	
T13B28	13	32.1																	
T13B29	18	32.5																	
T13B30	21	31.6			3														3
T13B31	6	31.2																	
T13B32	10	31.7																	
T13B33	4	33.3																	
T13B34	8	32.5																	
T13B35	23	33.1																	
T13B36	25	32.5																	
T13B37	14	33.0																	
T13B38	5	30.5																	
T13B39	13	32.1																	
T13B40	3	32.6																	
T13B41	15	32.3			3														
T13B42	11	32.0																	
T13B43	18	32.8																	
T13B44	3	32.3																	
T13B45	6	32.8																	

-- TAPE=13 --

ID	OUTCOME	TEMP	SETUP	LAUNCH	LAMELLA	IRREG	RHOSPECK	PHISPECK	RHO1	PHI1	RHO2	PHI2	ROUND1	ROUND2	ROUND3	ROUND4	ROUND5	BAND	RECERROR
T13B46	14	33.2		1															
T13B47	20	33.0																	
T13B48	2	32.5																	
T13B49	14	33.6																	
T13B50	16	32.9																	
T13B51	14	33.2				4	338	3.93					470						
T13B52	6	31.9																	
T13B53	10	33.3				5							383						
T13B54	15	33.5			3														
T13B55	18	33.5											338						
T13B56	22	32.6																	
T13B57	2	32.5																	
T13B58	12	33.6																	
T13B59	22	33.2																	
T13B60	21	33.3																	
T13B61	11	32.4																	
T13B62	16	33.7																	
T13B63	24	33.3				5													
T13B64	10	33.7																271	
T13B65	6	33.3		1															
T13B66	24	33.6																	
T13B67	4	33.4																271	
T13B68	3	33.5																271	
T13B69	10	33.9			3														
T13B70	18	33.7																	
T13B71	24	33.1																232	
T13B72	12	33.7		1															
T13B73	7	33.9											404	292	271	238	205		

-- TAPE=14 --

ID	OUTCOME	TEMP	SETUP	LAUNCH	LAMELLA	IRREG	RHOSPECK	PHISPECK	RHO1	PHI1	RHO2	PHI2	ROUND1	ROUND2	ROUND3	ROUND4	ROUND5	BAND	RECERROR
T14B01	13	30.7		1									470					338	
T14B02	4	32.2																	
T14B03	17	32.6																	
T14B04	11	32.8																	
T14B05	9	33.9																	
T14B06	18	33.3																	
T14B07	10	32.7																	
T14B08	11	33.8																	
T14B09	24	33.7																	
T14B10	3	33.2																232	3
T14B11	12	33.6																	
T14B12	14	33.4											338						
T14B13	21	33.3																	
T14B14	20	33.2											271						
T14B15	11	32.6		2															
T14B16	22	33.4																	
T14B17	11	32.9																	
T14B18	21	33.5																	
T14B19	3	32.7			2														
T14B20	4	33.2																	
T14B21	13	34.0											383						
T14B22	16	33.8																	
T14B23	12	33.4																	
T14B24	26	33.3		1															
T14B25	9	33.6																	
T14B26	13	33.6																	
T14B27	15	34.0																	
T14B28	24	33.2																	
T14B29	19	33.7																	
T14B30	18	33.2		2															
T14B31	10	33.0																	
T14B32	20	34.1			3														
T14B33	17	33.7																	
T14B34	20	33.6																	5
T14B35	12	33.1											404						
T14B36	24	33.5		1															
T14B37	11	33.7																	
T14B38	26	33.0				4	417	5.93											
T14B39	19	32.5											258						
T14B40	15	32.9																	
T14B41	8	33.2																	
T14B42	21	33.1																	
T14B43	22	32.7																	
T14B44	19	32.8				4	437	0.00											
T14B45	8	32.1																	

TAPE=14

ID	OUTCOME	TEMP	SETUP	LAUNCH	LAMELLA	IRREG	RHOSPECK	PHISPECK	RHO1	PHI1	RHO2	PHI2	ROUND1	ROUND2	ROUND3	ROUND4	ROUND5	BAND	RECERROR
T14B46	16	33.0																	
T14B47	2	33.5																	
T14B48	3	33.0				4	338	0.00											
T14B49	1	33.0											292						
T14B50	17	33.3																	
T14B51	19	33.2																	
T14B52	11	32.9																	3
T14B53	22	33.4																238	
T14B54	14	32.5																	
T14B55	17	32.5																	
T14B56	6	33.4																	
T14B57	11	33.6		1									470	205					
T14B58	2	33.6																	
T14B59	16	32.8			2														
T14B60	17	33.5			1														
T14B61	10	33.5																	
T14B62	23	32.8																	
T14B63	21	32.8																	
T14B64	18	32.7																	
T14B65	1	32.8			1														
T14B66	23	33.8							404	0.79									
T14B67	2	32.4																	

TAPE=15

ID	OUTCOME	TEMP	SETUP	LAUNCH	LAMELLA	IRREG	RHOSPECK	PHISPECK	RHO1	PHI1	RHO2	PHI2	ROUND1	ROUND2	ROUND3	ROUND4	ROUND5	BAND	RECERROR
T15B01	22	29.0		2		4	383	5.50										470	
T15B02	22	29.5			3													470	
T15B03	15	30.0				6							417					292	
T15B04	8	29.3				5							383	292					
T15B05	2	30.1																	
T15B06	24	31.3				5												338	
T15B07	21	31.3																	
T15B08	5	31.4																	
T15B09	21	31.4																	
T15B10	3	30.9											404						
T15B11	25	32.0																	
T15B12	25	32.2																	
T15B13	12	31.6																	
T15B14	18	32.9																	
T15B15	23	31.4											383						
T15B16	26	32.0																	
T15B17	17	33.3																	
T15B18	19	32.7		1															
T15B19	15	32.0																	
T15B20	3	32.7																	
T15B21	2	32.5																	
T15B22	11	33.1		1															
T15B23	17	32.4																	
T15B24	9	33.1											338	271					
T15B25	26	32.9																	
T15B26	20	32.5				5													
T15B27	19	32.0				4	437	4.71											
T15B28	22	31.3																	
T15B29	18	32.0																	
T15B30	13	32.4																	
T15B31	3	32.5				2													
T15B32	8	33.0																	
T15B33	14	33.1																	
T15B34	15	32.8			3	4	383	5.50											
T15B35	9	32.3			2														
T15B36	6	33.6		1															
T15B37	13	33.1																	
T15B38	8	32.5				2													
T15B39	21	33.8																	
T15B40	16	33.5																	3
T15B41	10	31.0				3													
T15B42	16	31.8		1															
T15B43	11	33.0																	
T15B44	15	33.0																	
T15B45	12	33.6																	

TAPE=15

ID	OUTCOME	TEMP	SETUP	LAUNCH	LAMELLA	IRREG	RHOSPECK	PHISPECK	RHO1	PHI1	RHO2	PHI2	ROUND1	ROUND2	ROUND3	ROUND4	ROUND5	BAND	RECERROR
T15B46	16	33.4			3														
T15B47	25	32.5																	
T15B48	23	33.4																	
T15B49	9	32.9																	
T15B50	3	34.1																	
T15B51	25	33.6																	
T15B52	10	33.4																	
T15B53	4	33.7																	
T15B54	10	33.4																	
T15B55	11	34.3																	
T15B56	9	34.2																	
T15B57	10	32.8																	
T15B58	15	33.6																	
T15B59	5	34.1		1															
T15B60	23	33.5																258	
T15B61	21	33.8											364					271	
T15B62	11	33.2		2		5													
T15B63	13	34.1																	
T15B64	3	33.7											470						
T15B65	18	33.6			3														
T15B66	3	32.9																	
T15B67	2	33.4																	
T15B68	14	33.8			3														
T15B69	23	33.9																	
T15B70	16	32.8																	
T15B71	18	34.2																	
T15B72	15	33.2		1														238	
T15B73	23	34.4																	
T15B74	26	33.5		2															
T15B75	15	34.2																	3
T15B76	11	34.3																	
T15B77	16	34.6																	

D Example graphs

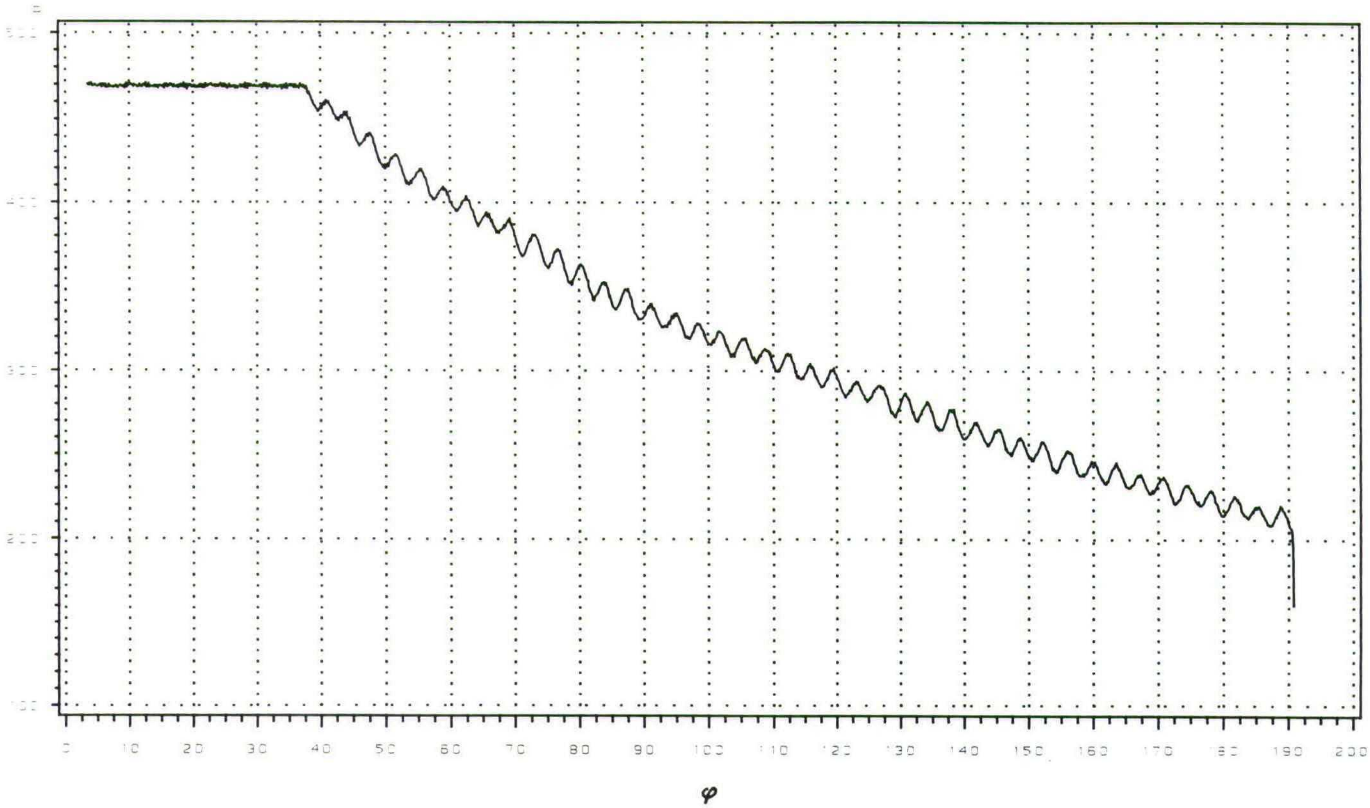

T10B03

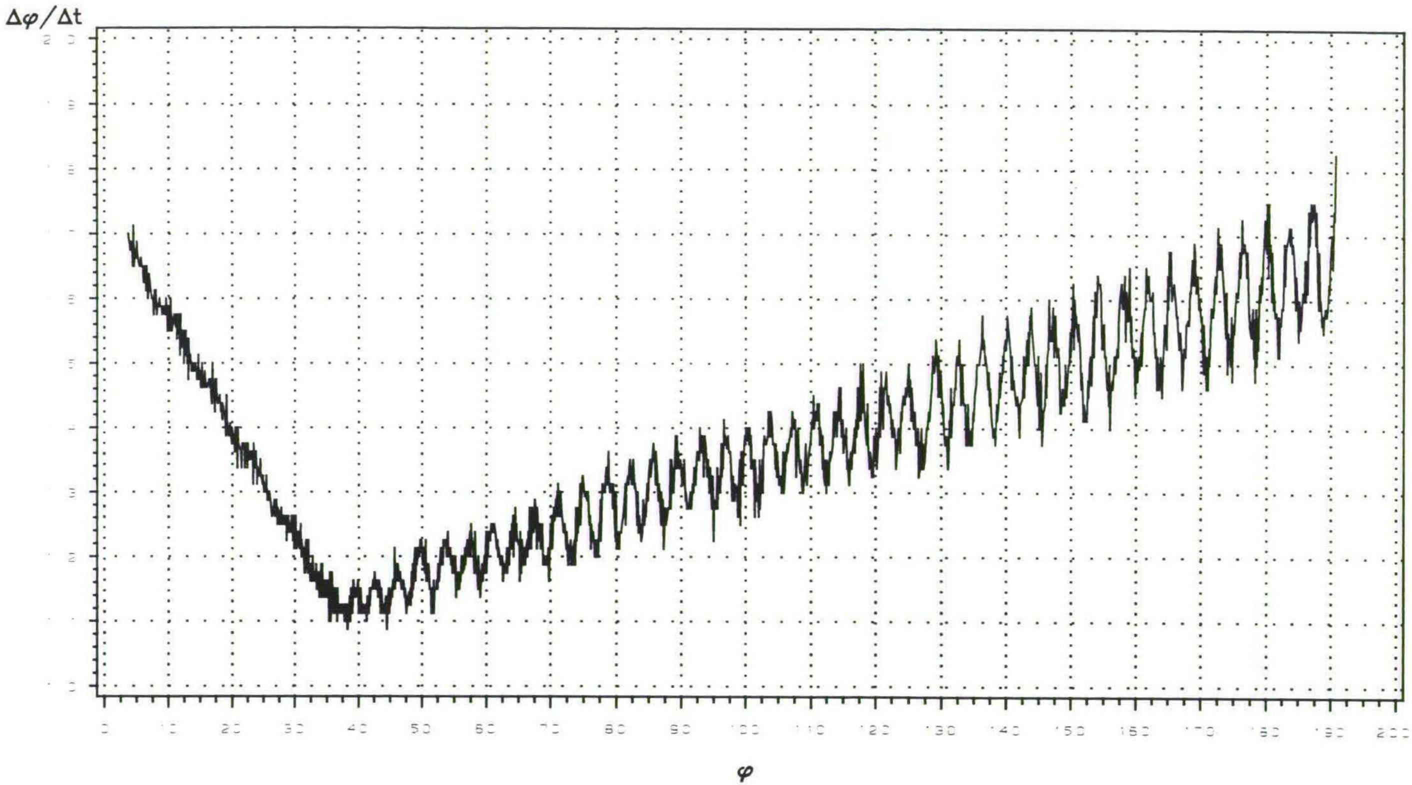
Δφ/Δt
φ

E Example file

0.00	470.178	3.561
0.08	469.873	3.697
0.16	470.391	3.832
0.24	470.126	3.966
0.32	470.697	4.101
0.40	469.440	4.235
0.48	469.428	4.367
0.56	469.585	4.504
0.64	469.826	4.636
0.72	469.478	4.770
0.80	469.125	4.903
0.88	469.093	5.038
1.04	469.685	5.303
1.12	469.824	5.435
1.20	470.090	5.567
1.28	468.837	5.700
1.36	469.218	5.832
1.44	470.095	5.964
1.52	469.711	6.094
1.60	468.971	6.225
1.68	469.855	6.357
1.76	468.389	6.486
1.84	468.890	6.618
1.92	468.722	6.746
2.00	469.907	6.875
2.08	468.955	7.006
2.24	468.843	7.264
2.32	468.729	7.392
2.40	468.344	7.520
2.48	468.865	7.646
2.56	468.889	7.775
2.64	468.964	7.902
2.72	469.330	8.031
2.80	468.679	8.157
2.88	468.225	8.284
2.96	468.846	8.411
3.04	469.402	8.539
3.12	469.575	8.666
3.20	469.186	8.793
3.28	468.918	8.919
3.44	469.136	9.173
3.52	468.085	9.299
3.60	469.704	9.425
3.68	470.477	9.553
3.76	468.518	9.680

133.84	212.705	186.312
133.92	211.701	186.441
134.00	210.636	186.580
134.08	209.255	186.715
134.16	209.091	186.853
134.24	208.591	186.993
134.32	208.556	187.131
134.48	208.871	187.411
134.56	209.913	187.550
134.64	210.928	187.685
134.72	212.272	187.824
134.80	213.495	187.955
134.88	213.334	188.082
134.96	215.167	188.216
135.04	215.522	188.343
135.12	217.031	188.471
135.20	217.586	188.596
135.28	220.092	188.722
135.36	219.318	188.846
135.44	219.026	188.972
135.52	217.505	189.099
135.68	216.464	189.351
135.76	215.087	189.478
135.84	214.078	189.608
135.92	213.157	189.737
136.00	211.299	189.870
136.08	209.662	190.005
136.16	208.029	190.141
136.24	207.261	190.273
136.32	206.311	190.412
136.40	203.579	190.550
136.48	194.879	190.696
136.94	172.531	190.789
137.10	162.490	190.800
137.18	162.490	190.800
137.26	161.336	190.797
137.42	160.906	190.792
137.50	161.439	190.800
137.66	161.693	190.796
137.74	160.981	190.798
137.82	161.046	190.798
137.90	161.215	190.796
137.98	160.934	190.797
138.06	161.228	190.798
138.14	161.386	190.799
138.22	161.075	190.797
138.30	161.401	190.800
138.38	161.106	190.797

IN 1993 REEDS VERSCHENEN

588 Rob de Groof and Martin van Tuijl
The Twin-Debt Problem in an Interdependent World
Communicated by Prof.dr. Th. van de Klundert

589 Harry H. Tigelaar
A useful fourth moment matrix of a random vector
Communicated by Prof.dr. B.B. van der Genugten

590 Niels G. Noorderhaven
Trust and transactions; transaction cost analysis with a differential behavioral assumption
Communicated by Prof.dr. S.W. Douma

591 Henk Roest and Kitty Koelemeijer
Framing perceived service quality and related constructs A multilevel approach
Communicated by Prof.dr. Th.M.M. Verhallen

592 Jacob C. Engwerda
The Square Indefinite LQ-Problem: Existence of a Unique Solution
Communicated by Prof.dr. J. Schumacher

593 Jacob C. Engwerda
Output Deadbeat Control of Discrete-Time Multivariable Systems
Communicated by Prof.dr. J. Schumacher

594 Chris Veld and Adri Verboven
An Empirical Analysis of Warrant Prices versus Long Term Call Option Prices
Communicated by Prof.dr. P.W. Moerland

595 A.A. Jeunink en M.R. Kabir
De relatie tussen aandeelhoudersstructuur en beschermingsconstructies
Communicated by Prof.dr. P.W. Moerland

596 M.J. Coster and W.H. Haemers
Quasi-symmetric designs related to the triangular graph
Communicated by Prof.dr. M.H.C. Paardekooper

597 Noud Gruijters
De liberalisering van het internationale kapitaalverkeer in historisch-institutioneel perspectief
Communicated by Dr. H.G. van Gemert

598 John Görtzen en Remco Zwetheul
Weekend-effect en dag-van-de-week-effect op de Amsterdamse effectenbeurs?
Communicated by Prof.dr. P.W. Moerland

599 Philip Hans Franses and H. Peter Boswijk
Temporal aggregration in a periodically integrated autoregressive process
Communicated by Prof.dr. Th.E. Nijman

600 René Peeters
On the p-ranks of Latin Square Graphs
Communicated by Prof.dr. M.H.C. Paardekooper

601 Peter E.M. Borm, Ricardo Cao, Ignacio García-Jurado
Maximum Likelihood Equilibria of Random Games
Communicated by Prof.dr. B.B. van der Genugten

602 Prof.dr. Robert Bannink
Size and timing of profits for insurance companies. Cost assignment for products with multiple deliveries.
Communicated by Prof.dr. W. van Hulst

603 M.J. Coster
An Algorithm on Addition Chains with Restricted Memory
Communicated by Prof.dr. M.H.C. Paardekooper

604 Ton Geerts
Coordinate-free interpretations of the optimal costs for LQ-problems subject to implicit systems
Communicated by Prof.dr. J.M. Schumacher

605 B.B. van der Genugten
Beat the Dealer in Holland Casino's Black Jack
Communicated by Dr. P.E.M. Borm

606 Gert Nieuwenhuis
Uniform Limit Theorems for Marked Point Processes
Communicated by Dr. M.R. Jaïbi

607 Dr. G.P.L. van Roij
Effectisering op internationale financiële markten en enkele gevolgen voor banken
Communicated by Prof.dr. J. Sijben

608 R.A.M.G. Joosten, A.J.J. Talman
A simplicial variable dimension restart algorithm to find economic equilibria on the unit simplex using n(n+1) rays
Communicated by Prof.Dr. P.H.M. Ruys

609 Dr. A.J.W. van de Gevel
The Elimination of Technical Barriers to Trade in the European Community
Communicated by Prof.dr. H. Huizinga

610 Dr. A.J.W. van de Gevel
Effective Protection: a Survey
Communicated by Prof.dr. H. Huizinga

611 Jan van der Leeuw
First order conditions for the maximum likelihood estimation of an exact ARMA model
Communicated by Prof.dr. B.B. van der Genugten

612 Tom P. Faith
Bertrand-Edgeworth Competition with Sequential Capacity Choice
Communicated by Prof.Dr. S.W. Douma

613 Ton Geerts
The algebraic Riccati equation and singular optimal control: The discrete-time case
Communicated by Prof.dr. J.M. Schumacher

614 Ton Geerts
Output consistency and weak output consistency for continuous-time implicit systems
Communicated by Prof.dr. J.M. Schumacher

615 Stef Tijs, Gert-Jan Otten
Compromise Values in Cooperative Game Theory
Communicated by Dr. P.E.M. Borm

616 Dr. Pieter J.F.G. Meulendijks and Prof.Dr. Dick B.J. Schouten
Exchange Rates and the European Business Cycle: an application of a 'quasi-empirical' two-country model
Communicated by Prof.Dr. A.H.J.J. Kolnaar

617 Niels G. Noorderhaven
The argumentational texture of transaction cost economics
Communicated by Prof.Dr. S.W. Douma

618 Dr. M.R. Jaïbi
Frequent Sampling in Discrete Choice
Communicated by Dr. M.H. ten Raa

619 Dr. M.R. Jaïbi
A Qualification of the Dependence in the Generalized Extreme Value Choice Model
Communicated by Dr. M.H. ten Raa

620 J.J.A. Moors, V.M.J. Coenen, R.M.J. Heuts
Limiting distributions of moment- and quantile-based measures for skewness and kurtosis
Communicated by Prof.Dr. B.B. van der Genugten

621 Job de Haan, Jos Benders, David Bennett
Symbiotic approaches to work and technology
Communicated by Prof.dr. S.W. Douma

622 René Peeters
Orthogonal representations over finite fields and the chromatic number of graphs
Communicated by Dr.ir. W.H. Haemers

623 W.H. Haemers, E. Spence
Graphs Cospectral with Distance-Regular Graphs
Communicated by Prof.dr. M.H.C. Paardekooper

624 Bas van Aarle
The target zone model and its applicability to the recent EMS crisis
Communicated by Prof.dr. H. Huizinga

625 René Peeters
Strongly regular graphs that are locally a disjoint union of hexagons
Communicated by Dr.ir. W.H. Haemers

626 René Peeters
Uniqueness of strongly regular graphs having minimal *p*-rank
Communicated by Dr.ir. W.H. Haemers

627 Freek Aertsen, Jos Benders
Tricks and Trucks: Ten years of organizational renewal at DAF?
Communicated by Prof.dr. S.W. Douma

628 Jan de Klein, Jacques Roemen
Optimal Delivery Strategies for Heterogeneous Groups of Porkers
Communicated by Prof.dr. F.A. van der Duyn Schouten

629 Imma Curiel, Herbert Hamers, Jos Potters, Stef Tijs
The equal gain splitting rule for sequencing situations and the general nucleolus
Communicated by Dr. P.E.M. Borm

630 A.L. Hempenius
Een statische theorie van de keuze van bankrekening
Communicated by Prof.Dr.Ir. A. Kapteyn

631 Cok Vrooman, Piet van Wijngaarden, Frans van den Heuvel
Prevention in Social Security: Theory and Policy Consequences
Communicated by Prof.Dr. A. Kolnaar

IN 1994 REEDS VERSCHENEN

632 B.B. van der Genugten
Identification, estimating and testing in the restricted linear model
Communicated by Dr. A.H.O. van Soest

633 George W.J. Hendrikse
Screening, Competition and (De)Centralization
Communicated by Prof.dr. S.W. Douma

634 A.J.T.M. Weeren, J.M. Schumacher, and J.C. Engwerda
Asymptotic Analysis of Nash Equilibria in Nonzero-sum Linear-Quadratic Differential Games. The Two-Player case
Communicated by Prof.dr. S.H. Tijs

635 M.J. Coster
Quadratic forms in Design Theory
Communicated by Dr.ir. W.H. Haemers

636 Drs. Erwin van der Krabben, Prof.dr. Jan G. Lambooy
An institutional economic approach to land and property markets - urban dynamics and institutional change
Communicated by Dr. F.W.M. Boekema

637 Bas van Aarle
Currency substitution and currency controls: the Polish experience of 1990
Communicated by Prof.dr. H. Huizinga

638 J. Bell
Joint Ventures en Ondernemerschap: Interpreneurship
Communicated by Prof.dr. S.W. Douma

639 Frans de Roon and Chris Veld
Put-call parities and the value of early exercise for put options on a performance index
Communicated by Prof.dr. Th.E. Nijman

640 Willem J.H. Van Groenendaal
Assessing demand when introducing a new fuel: natural gas on Java
Communicated by Prof.dr. J.P.C. Kleijnen

641 Henk van Gemert & Noud Gruijters
Patterns of Financial Change in the OECD area
Communicated by Prof.dr. J.J Sijben

642 Drs. M.R.R. van Bremen, Drs. T.A. Marra en Drs. A.H.F. Verboven
Aardappelen, varkens en de termijnhandel: de reële optietheorie toegepast
Communicated by Prof.dr. P.W. Moerland

643 W.J.H. Van Groenendaal en F. De Gram
The generalization of netback value calculations for the determination of industrial demand for natural gas
Communicated by Prof.dr. J.P.C. Kleijnen

644 Karen Aardal, Yves Pochet and Laurence A. Wolsey
Capacitated Facility Location: Valid Inequalities and Facets
Communicated by Dr.ir. W.H. Haemers

645 Jan J.G. Lemmen
An Introduction to the Diamond-Dybvig Model (1983)
Communicated by Dr. S. Eijffinger

646 Hans J. Gremmen and Eva van Deurzen-Mankova
Reconsidering the Future of Eastern Europe: The Case of Czecho-Slovakia
Communicated by Prof.dr. H.P. Huizinga

647 H.M. Webers
Non-uniformities in spatial location models
Communicated by Prof.dr. A.J.J. Talman

648 Bas van Aarle
Social welfare effects of a common currency
Communicated by Prof.dr. H. Huizinga

649 Laurence A.G.M. van Lent
De winst is absoluut belangrijk!
Communicated by Prof.drs. G.G.M. Bak

650 Bert Hamminga
Jager over de theorie van de internationale handel
Communicated by Prof.dr. H. Huizinga

651 J.Ch. Caanen and E.N. Kertzman
A comparison of two methods of inflation adjustment
Communicated by Prof.dr. J.A.G. van der Geld

652 René van den Brink
A Note on the τ-Value and τ-Related Solution Concepts
Communicated by Prof.dr. P.H.M. Ruys

653 J. Engwerda and G. van Willigenburg
Optimal sampling-rates of digital LQ and LQG tracking controllers with costs associated to sampling
Communicated by Prof.dr. J.M. Schumacher

Katholieke Universiteit Brabant
PO Box 90153
5000 LE Tilburg
The Netherlands